Carbohydrate Polymers 229 (2020) 115469

Contents lists available at ScienceDirect

Carbohydrate Polymers

journal homepage: www.elsevier.com/locate/carbpol

In vitro digestion of polysaccharide including whey protein isolate hydrogels

Baris Ozel[a,b], Ozlem Aydin[a], Mecit Halil Oztop[b,*]

[a] Food Engineering Department, Ahi Evran University, Kirsehir, Turkey
[b] Food Engineering Department, Middle East Technical University, Ankara, Turkey

ARTICLE INFO

Keywords:
Release
Whey protein
Hydrogel
Digestion
NMR
FTIR
SEM

ABSTRACT

Hydrogels are great systems for bioactive agent encapsulation and delivery. In this study, polysaccharide blended whey protein isolate (WPI) based hydrogels were loaded with black carrot (*Daucus carota*) concentrate (BC) and *in vitro* gastrointestinal release measurements were performed. Prior to 6 h digestion in simulated intestinal fluid (SIF), all hydrogels were exposed to simulated gastric fluid (SGF) for 2 h. Pectin (PC), gum tragacanth (GT) and xanthan gum (XG) were the polysaccharides used with WPI to manipulate the release behavior. Physico-chemical changes of the hydrogels throughout the digestion were evaluated by Fourier transform infrared (FTIR) spectroscopy and nuclear magnetic resonance (NMR) relaxometry measurements. Each polysaccharide induced different physico-chemical interactions within the hydrogels due to their distinct structural characteristics. Polysaccharide blending to hydrogels also retarded the release rates in all samples in SIF ($p < 0.05$). Moreover, microstructural differences between hydrogels were evaluated by scanning electron microscope (SEM) images.

1. Introduction

Protein based delivery systems for encapsulation of bioactive compounds have gained growing interest in recent years. Functional attributes of proteins including surface activity, gelling ability and high interacting capability of the functional groups located on their surfaces, offer a great opportunity for the delivery of bioactive agents (McClements & Gumus, 2016). Thermal denaturation of proteins is widely utilized to form hydrogels for such delivery purposes and one of the most suitable proteins are whey proteins (Gunasekaran, Ko, & Xiao, 2007). Above 70 °C, whey proteins experience a thermal denaturation creating a three-dimensional gel network (Munialo et al., 2016).

Globular proteins found in whey, including β-lactoglobulin (β-Lg), α-lactalbumin (α-LA) and bovine serum albumin (BSA), are the main agents contributing to heat induced gelling of WPI (Fathi, Donsi, & McClements, 2018; Takagi, Teshima, Okunuki, & Sawada, 2003). Among them, as the major protein in whey, β-Lg dominates the total gelling mechanism of WPI (Hoffman & Van Mil, 1999). In contrast to β-Lg, α-LA cannot polymerize by itself when heated above 70 °C (De la Fuente, Singh, & Hemar, 2002). Addition of β-Lg allows interactions between α-LA and itself through disulfide bridges. Heating of α-LA, β-Lg and BSA accelerates aggregation rate thus promotes a synergistic effect on aggregation (Havea, Singh, & Creamer, 2001). Thermal heat induced denaturation steps of β-Lg mainly consists of initial denaturation (unfolding) and subsequent aggregation stages (Prabakaran & Damodaran, 1997).

In this study, PC, GT and XG polymers were combined with WPI in order to design hydrogels with different release characteristics. To the best of our knowledge, there are no studies characterizing combination of PC, GT and XG with WPI hydrogels in SIF conditions. PC, GT and XG differ from each other in many ways such as viscosity increasing, charge density and emulsifying abilities. PC is an anionic, covalently linked galacturonic acid containing heteropolysaccharide and naturally found in primary cell walls of most plants (Ventura & Bianco-Peled, 2015). Approximately 70% of PC is composed of galacturonic acid units and the pKa of the PC is around 2.9 to 3.2 close to the pKa value of the monomeric galacturonic acid. Homogalacturonic regions of PC is interrupted by rhamnogalacturonic regions in which hydrophilic side chains including neutral sugars carried by α-L-rhamnopyranosyl residues (Ralet, Dronnet, Buchholt, & Thibault, 2011). PC is commonly used in food industry for its gelling and stabilizing abilities (Mohnen, 2008). XG is also an anionic biodegradable polymer widely used in food industry as a thickening agent. The main chain of XG molecule consists of β-D-glucose units and the chemical structure of this chain is identical to that of cellulose. XG structure also contains repeated trisaccharide side chains linked to main cellulosic backbone. These side chains are composed of one D-glucuronic acid unit between two D-mannose units. The terminal D-mannose unit contains a pyruvic acid residue whereas

* Corresponding author at: Middle East Technical University, Universiteler Mah, Dumlupinar Bulvari, No: 1 Cankaya, 06800, Ankara, Turkey.
E-mail address: mecit@metu.edu.tr (M.H. Oztop).

https://doi.org/10.1016/j.carbpol.2019.115469
Received 5 July 2019; Received in revised form 7 October 2019; Accepted 11 October 2019
Available online 19 October 2019
0144-8617/

the first D-mannose unit linked to the main chain has an acetyl group. The presence of these groups on the side chains, contributes to the strong anionic characteristic of the XG molecule (García-Ochoa, Santos, Casas, & Gómez, 2000). XG, as a heteropolysaccharide with relatively high molecular weight (~2000 kDa), is used in a wide range of food products as emulsion stabilizer and texture regulator. In its native state, XG adopts a double stranded helix conformation in solutions leading to an increase in the viscosity of that solution even at very low concentrations (Mikac, Sepe, Kristl, & Baumgartner, 2010). GT, on the other hand, is a highly branched, acid resistant and anionic polysaccharide with high water binding ability due to the presence of D-galacturonic acid, D-galactose, D-xylose, L-arabinose and L-fucose units in its structure (Mostafavi, Kadkhodaee, Emadzadeh, & Koocheki, 2016). GT has a pKa around 3.0 and the negative character of the polysaccharide mainly originates from its carboxyl group which is in galacturonic acid (Nur, Ramchandran, & Vasiljevic, 2016; Yokoyama, Srinivasan, & Fogler, 1988). Two main fractions comprising the chemical structure of GT are tragacanthin which is a water soluble fraction giving the polysaccharide its liquid character and bassorin which generates the swelling and gel forming ability of the gum (Balaghi, Mohammadifar, Zargaraan, Gavlighi, & Mohammadi, 2011). While bassorin is a complex structure because of the presence of polymethoxylated acids, tragacanthin comprises the demethoxylated portion of these compounds (Balaghi, Mohammadifar, & Zargaraan, 2010).

Black carrot concentrate (BC) is an important source of polyphenols especially flavonoids (Akhtar et al., 2017). These flavonoids are reported to have a protective role against several degenerative diseases such as diabetes, cancer, oxidative stress, neuro-degeneration and cardiovascular diseases (Arts & Hollman, 2005; Graf, Milbury, & Blumberg, 2005; Metzger & Barnes, 2009). BC differs from most of the other plant flavonoid sources with its high anthocyanin content (1.75 g/kg) and remarkable anthocyanin profile (Akhtar et al., 2017; Kirca, Ozkan, & Cemeroglu, 2006). Anthocyanin pigments are water soluble and give black carrots their purple color (Yildiz, 2010). Therefore, commercial BC anthocyanins are widely used as natural food colorants in food industry (Downham & Collins, 2000). However, the susceptibility of anthocyanin colorants obtained from various sources to external conditions including temperature and pH changes, limits their use in food manufacturing processes (Betz & Kulozik, 2011). Most of the BC anthocyanins are acylated mainly in cyanidin 3-sinapoyl-xylosyl-glucosyl-galactoside and cyanidin 3-feruloyl-xylosyl-glucosyl-galactoside forms (Kirca et al., 2006; Stintzing, Stintzing, Carle, Frei, & Wrolstad, 2002). Due to their higher acylated anthocyanin content than other fruit or vegetable anthocyanins, BC anthocyanins are more stable over a wider pH range as well as at higher temperatures (Ersus Bilek, Yılmaz, & Özkan, 2017; Kammerer, Carle, & Schieber, 2004). Kirca et al. (2006) reported that BC anthocyanins had high heat stability in apple and grape juices even at 90 °C (Kirca et al., 2006). These characteristics of BC anthocyanins enable their encapsulation in heat induced WPI hydrogels for controlled release purposes. Additionally, at high concentrations, anthocyanins increase their stability through their self-association in thermally generated whey protein gel matrices (Betz & Kulozik, 2011; Naczk, Grant, Zadernowski, & Barre, 2006). Encapsulated active agents in polymer networks were used for nutraceutical delivery systems before and BC could also be used for such purposes (Pakzad, Alemzadeh, & Kazemi, 2013).

Encapsulation of BC in delivery matrixes is necessary particularly for gastrointestinal digestion. Kamiloglu, Pasli, Ozcelik, Van Camp, and Capanoglu (2015) demonstrated that total phenolic content of black carrot jams and marmalades were significantly lowered in gastrointestinal digestion conditions (Kamiloglu et al., 2015). Total polyphenol, flavonoid and anthocyanin contents further decrease during transition from the acidic gastric environment to mildly alkaline intestinal medium. Especially anthocyanins are highly unstable at intestinal pH (McDougall, Dobson, Smith, Blake, & Stewart, 2005; Tagliazucchi, Verzelloni, Bertolini, & Conte, 2010). Although in vitro gastrointestinal studies offer a limited assessment for gastrointestinal models due to some hindrances such as a static digestion process, these studies provide valuable and practical information for respective human and animal gastrointestinal models which are difficult to set up (Bouayed, Hoffmann, & Bohn, 2011). Moreover, evaluation of in vitro models could be correlated with human and animal models (Biehler & Bohn, 2010).

In our previous study, release behaviors of these hydrogels were characterized only in SGF and comparisons regarding the physicochemical changes were made between the native state of the hydrogels and SGF treated ones, in the absence of SIF treatment (Ozel, Aydin, Grunin, & Oztop, 2018). The main objective of this study was to investigate the release behaviors of PC, GT and XG blended, BC loaded, heat induced WPI hydrogels in gastrointestinal conditions. Physicochemical changes within the hydrogel matrices were also analyzed via nuclear magnetic resonance (NMR) relaxometry and Fourier transform infrared (FTIR) spectroscopy measurements. Since NMR relaxometry is a nondestructive technique and has the ability to detect molecular motions in the millisecond range, transverse relaxation time (T_2) experiments were performed to understand the interactions between liquid release media, encapsulated bioactive agent and polymer matrices comprising the hydrogels (Oztop, McCarthy, McCarthy, & Rosenberg, 2014; Vittadini, Dickinson, & Chinachoti, 2002). FTIR spectroscopy has been extensively used for structural composition analysis of food components (Dong et al., 1996; Ebrahimi, Koocheki, Milani, & Mohebbi, 2016). In addition to NMR relaxometry and FTIR spectroscopy analyses, scanning electron microscope (SEM) images were examined to observe the resulting microstructural changes due to the gastrointestinal digestion of the hydrogels.

2. Materials and methods

2.1. Materials

WPI was purchased from Hardline Nutrition (Kavi Food Ltd. Co., Istanbul, Turkey) and its protein content was determined by Kjeldahl method as 88.5% (w/w). Polysaccharides PC (Product Code: GP 1507, FMC, Italy S.R.L.) and GT from *Astragalus gummifier* Labillardiere (Product Code: TRA5183, Thew Arnott & Co. Ltd, Deeside, United Kingdom) and xanthan gum (XG) from *Xanthomonas campestris* were used as the additional polymers in the gels. Pectin was a high methoxy pectin extracted from citrus peel and had an esterification degree of 64–68%. XG was purchased from a local company (Smart Kimya Tic. ve Danismanlik Ltd. Sti., Izmir, Turkey). Sodium azide was used to protect hydrogels from microbial activity (Merck KgaA, Darmstadt, Germany). FTIR spectra of all polysaccharides in their native form showed a characteristic absorption region between 950 and 1200 cm^{-1} which is a fingerprint for carbohydrates (see the supplementary file for FTIR spectra of polysaccharides). PC used in this study having a higher absorption peak at 1750 cm^{-1} than 1650 cm^{-1} was a high methoxyl pectin since peak at 1650 cm^{-1} represents free carboxyl groups whereas 1750 cm^{-1} indicates the presence of esterified groups (Urias-Orona et al., 2010). Compositional analysis of GT was conducted in a previous study and it revealed the presence of 60% tragacanthin and 40% bassorin (w/w) which are water soluble and water insoluble parts in the GT physical mixture, respectively (Pocan, Ilhan, & Oztop, 2019). Peak around 1620 cm^{-1} in the GT spectrum showed the presence of protein residues in the GT powder used in this study (Kurt, 2018). More compact and branched structure of XG restricted the molecular vibrations within the XG molecule and this resulted in lower absorption values despite similar peak patterns with the other polysaccharides. A more distinct peak around 1410 cm^{-1} in XG FTIR spectrum with respect to PC and GT proved the existence of symmetric vibrations caused by carboxyl groups in the pyruvate and glucuronate (Lal, Dubey, Gaur, Verma, & Verma, 2017). BC (black carrot concentrate) was provided by Targid A.S. (Targid Agriculture Co., Inc., Icel, Turkey). Total phenolic

content of BC was measured as 20.59 mg of Gallic Acid Equivalent (GAE) / g sample by Folin-Ciocalteu method (Arab, Alemzadeh, & Maghsoudi, 2011; Dag, Kilercioglu, & Oztop, 2017). The antioxidant activity of BC was found as 1.93 mg 2,2-diphenyl-1-picrylhydrazyl (DPPH) / g sample by DPPH radical scavenging method (Wang, Gao, Zhou, Cai, & Yao, 2008). Pepsin and pancreatin enzymes were used for SGF and SIF preparations, respectively (Sigma-Aldrich Co., St. Louis, MO). Sodium chloride (NaCl, Sigma-Aldrich Co., St. Louis, MO) was added to SGF formulation whereas monobasic potassium phosphate (KH_2PO_4, Merck KgaA, Darmstadt, Germany) was put in SIF solution.

2.2. Sample and release media preparations

Hydrogel solutions were formulated mainly by WPI 15% (w/w) and 0.5% (w/w) blended polymer (PC, GT or XG). C samples did not contain any additional polymer. All hydrogel formulations included 4% (w/w) BC as the bioactive agent and 0.02% (w/w) sodium azide along with WPI as the antimicrobial agent. Both polysaccharide solutions including BC and WPI solutions stirred separately, at 15 000 rpm for 2 min with Ultra Turrax T-18 (IKA Corp., Staufen, Germany). Then, these solutions were combined for overnight stirring at room temperature. Only XG containing solutions were centrifuged at 715 *g* for 2 min prior to combination with the WPI solution in order to remove air bubbles formed in the solution (Hanil Science Industrial Co., Ltd., Incheon, Korea). After complete mixing, hydrogel solutions were poured into the cylindrical tubes having 5 cm length and 1.5 cm outer diameter. These tubes were put into a water bath for gelling (30 min, 90 °C). Before removing the hydrogels from the glass tubes, 15 min ice cooling was implemented. Obtained hydrogels were cut into smaller cylindrical shapes having 1.3 cm diameter and 2 cm length. SGF and SIF were used as release media. For the SGF preparation, the method used by Sarkar, Goh, Singh, and Singh (2009) was chosen (Sarkar et al., 2009). Finally, pH of the SGF was adjusted to 1.2. SIF was prepared as described in the United States Pharmacopoeia (24th edition, p 2236) and implemented by Takagi et al. (2003). pH of SIF was checked to obtain a final value around 6.8.

2.3. Monitoring in vitro release of black carrot concentrate in gastrointestinal fluids

Firstly, hydrogels having cylindrical shape (1.3 cm diameter, 2 cm length) were immersed into 40 ml SGF (pH 1.2, 37 °C) stirring at 80 rpm for 2 h. 4 ml of aliquots were taken from the SGF at specified time intervals and put back into the release medium after absorbance measurements in order to keep the volume constant. Absorbance values were measured at 530 nm with a UV–vis spectrophotometer (Mecasys Co. Ltd., Korea). A calibration curve (y = 7.5704x – 4E-5, where x and y represents g BC/40 g SGF and absorbance value, respectively) was previously prepared by correlation of known amounts of BC with their absorbance value at 530 nm (Bateman, Ye, & Singh, 2011). After 2 h gastric digestion, gel samples were removed from SGF and immediately put into SIF (pH 6.8, 37 °C, stirring at 80 rpm). Release in SIF was monitored for 6 h and 2.5 ml of aliquots were withdrawn from the medium in 1 h intervals and again poured back into medium. For the absorbance measurements wavelength of 545 nm was used and a calibration curve was also prepared for these measurements (y = 6.2821x – 7.2E-3, where x and y represented g BC/40 g SIF and absorbance value, respectively) (Takagi et al., 2003). Temperature of simulated gastrointestinal fluids were maintained at 37 °C throughout the experiment for simulating the real gastrointestinal conditions.

2.4. Soluble protein content measurements

As hydrogels are exposed to enzymes in digestive fluids protein loss is inevitable. Protein contents of hydrogels during digestion were determined in both SGF and SIF media according to the method determined by Lowry, Rosebrough, Farr, and Randall (1951) which is mainly based on the reaction of proteins with copper ions at alkaline conditions (Lowry et al., 1951). For the determination of protein contents in the release media, a calibration curve was prepared by the dilution of 1 mg/ml BSA stock solution in different ratios by distilled water (y = 1.6854x + 0.1027, where x and y represent BSA mg/ml and absorbance value, respectively). Since the enzyme concentrations were constant for respective digestion media, effects of enzymes on soluble protein content measurements in each digestion medium were considered as constant.

2.5. Nuclear magnetic resonance relaxometry measurements

Spin-spin ^1H relaxation measurements (T_2) of the hydrogels were measured by a 0.32 T benchtop NMR spectrometer equipped with a 16 mm probe (Spin Track SB4, Mary El, Russian Federation). Carr-Purcell-Meiboom-Gill (CPMG) sequence was used for the measurements. Decay curves were best described by monoexponential fitting (see the supplementary file for the decay curves of digested samples). Sequence parameters were set as 400 echoes with 1 ms echo time, 3000 ms repetition time (to assure complete recovery of the longitudinal magnetization) and 64 scans. T_2 values of the samples were measured right after SGF treatment and during SIF exposure, SIF measurements were taken in 2 h intervals (2, 4 and 6 h in SIF release). In addition to T_2 experiments, relative percent crystallinity values of the samples were measured to observe changes in the crystal polymorphism induced by gastrointestinal digestion. A 20.34 MHz NMR system (Spin Track, Resonance Systems GmbH, Kirchheim/Teck, Germany) with 10 mm probe diameter was used for the crystallinity measurements and Magic Sandwich Echo (MSE) sequence was used (Rhim, Pines, & Waugh, 1971). The instrument was equipped with a 10 mm radio-frequency (rf) coil. Duration of the 90° radio-frequency (rf) pulse was 2.4 μs. 10 μs interpulse time was chosen while the probe ringing time was detected as 9 μs. For each measurement 4 phase cycling steps were performed with 10 s repetition delay. The special module on the Relax8 software (Resonance Systems GmbH, Kirchheim/Teck, Germany) was used to calculate relative percent crystallinity values of the hydrogels. Crystallinity values are obtained using the 2nd moments as explained in the study of Grunin, Oztop, Guner, and Baltaci (2019). This approach does not require a multiparameter fitting and uses a simpler approach as described in the related reference. Before crystallinity analysis, hydrogels were dried at 65 °C for 1 day, in order to eliminate the excess moisture since presence of high amount of liquid dominates the obtained signal and makes it impossible to detect the signal coming from the crystalline region. All CPMG and MSE measurements were performed at room temperature (~25 °C) and hydrogels were cut longitudinally at 1.2 cm length and put into the test tubes in order to obtain sufficient signal to noise ratio. Since digestion experiments were performed at 37 °C and the rf probe could not be heated to 37 °C, all samples were left to equilibrate with the room temperature before measurements.

2.6. Fourier transform infrared spectroscopy measurements

IR Affinity-1 Spectrometer with attenuated total reflectance (ATR) attachment (Shimadzu Corporation, Kyoto, Japan) was used to analyze FTIR absorption spectra of hydrogels after SGF and complete gastrointestinal (SGF + SIF) digestions. Prior to FTIR analysis, hydrogels were frozen in −20 °C and then freeze-dried (Zhejiang Value Mechanical & Electrical Products Co. Ltd., Wenling City, China) for 2 days. Freeze-dried samples were then ground to powder form. The measurement range was 4000–500 cm^{-1}. 32 scans and 4 cm^{-1} resolution were implemented for the measurements. In addition to FTIR spectra of SGF and SIF treated hydrogels in the text, FTIR spectra of powder polysaccharides and hydrogels prior to digestion were also provided in the supplementary file.

2.7. Textural measurements

A texture analyzer equipped with a 50 N load cell and 1 cm diameter cylindrical stainless-steel probe (TA Plus Lloyd Instruments, U.K.) was used to measure the hardness values of the hydrogels. Hydrogels after SGF treatment and overall digestion (SGF + SIF) were subjected to hardness test. In addition, hardness values of hydrogels which were not immersed to the release media were also determined. During the compression test of the cylindrical samples a preload stress of 0.1 N and a stress speed of 100 mm/min were implemented. Two compression cycles (0.68 cm first extension and 0 cm second extension) with 100 mm/min test extension rate were applied. The maximum force generated due to the resistance to the first compression of the sample was defined as hardness (Zand-Rajabi & Madadlou, 2016).

2.8. Release experiments in simulated intestinal fluid (SIF)

Release data of hydrogels in SIF were plotted in the form of M_t/M_∞ vs time (h) to collect information on the unusual release behaviors of hydrogels in SIF. M_t denotes the measured amount of BC (g) in SIF at time t, M_∞ is the amount of BC in SIF at equilibrium.

2.9. Weight loss determination of hydrogels in simulated intestinal fluid

When exposed to SIF, all hydrogels eroded to some extent, thus weights of the samples were measured before and after SIF treatment. Weight loss ratios were calculated as;

$$\text{Weight loss (\%)} = ((W_{2\,h} - W_{8h})/W_{2\,h}) \times 100 \quad (1)$$

where W_{2h} is the weight of the sample after SGF treatment (in the beginning of SIF treatment) and W_{8h} denotes the final weight of the sample after the whole digestion (2 h SGF and subsequent 6 h SIF treatment).

2.10. Scanning Electron microscopy experiments

Initially, SGF and SIF treated hydrogels were kept frozen for 2 days. Then, these hydrogels were freeze dried (Zhejiang Value Mechanical & Electrical Products Co. Ltd., Wenling City, China). Freeze dried hydrogels were coated with thin layer of gold prior to SEM analyses. Analyses were conducted in Metallurgical and Materials Engineering Laboratory of METU, Ankara, Turkey. Images were captured at an accelerating voltage of 5–20 kV and 10000X magnification level was used (FEI Nova NanoSEM 430, Oregon, USA).

2.11. Statistical analysis

Differences between the measurements regarding hydrogel characteristics were analyzed by analysis of variance (ANOVA) with MINITAB (version 16). Tukey's test with 5% significance level ($p < 0.05$) was used to compare the means of the measurements. Each measurement was performed in triplicate.

3. Results and discussion

3.1. Release profiles

Cumulative release profiles in gastrointestinal digestion for 8 h revealed that both type of the release medium and blending of the polymer affected the release characteristics of hydrogels (Fig. 1). Generally, hydrogels experienced faster release rates in SGF and gradual BC release in SIF. After initial SGF treatment for 2 h, PC hydrogels attained a higher release rate (83%) whereas C, XG and GT samples retarded BC release (67–61%) in highly acidic pH around 1.2 with respect to PC samples ($p < 0.05$). Electrical charges on the WPI and blended

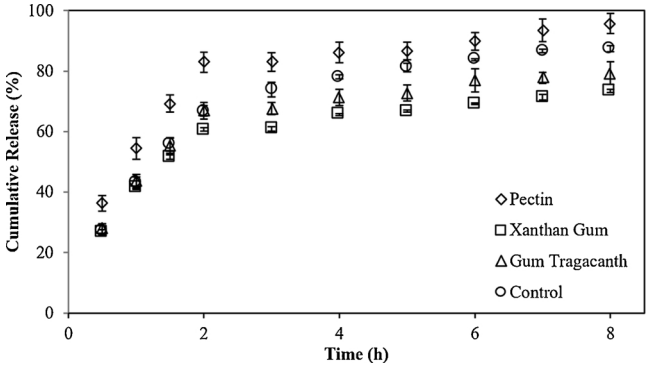

Fig. 1. Cumulative BC release profiles of polymer blended (pectin, gum tragacanth, xanthan gum) and sole WPI (control) hydrogels in gastrointestinal digestion. Errors are represented as standard errors.

polysaccharide molecules, thus the electrostatic interactions between proteins and polysaccharides are highly dependent on the changes in pH (Santipanichwong, Suphantharika, Weiss, & McClements, 2008). At very low pH environment of SGF, both the ionizable groups of WPI (pI ~ 5.2) and polymers (pKa ~ 3.0) were suppressed due to the excess protonation (Ozel, Cikrikci, Aydin, & Oztop, 2017). The extent of protonation is related to the charge density of the polymers (Belscak-Cvitanovic et al., 2015). With its relatively lower molecular weight (~100 kDa) and more linear structure compared to other blended polymers, PC is expected to have a lower charge density with respect to GT and XG molecules (Mohnen, 2008; Zhang, Zhang, & Vardhanabhuti, 2014). Therefore, carboxylic groups of PC were not dissociated, almost complete protonation of PC molecule was achieved and negatively charged portions on the PC molecule were eliminated that would otherwise contribute to the crosslinking within the hydrogel matrix. Charge repulsion was the dominant mechanism in the PC added WPI hydrogels. In contrast, abundance of negatively charged side groups of especially XG, made it difficult to protonate all groups even at SGF conditions and remaining negatively charged portions of the GT and XG molecules contributed to further crosslinking. Due to these properties, GT and XG were declared as acid stable polymers while PC was susceptible to high acidity (Balaghi et al., 2011; Fabek, Messerschmidt, Brulport, & Goff, 2014; Saldamli, 1998) Moreover, even C samples with no additional polymer, did not attain as high release rates as PC samples in SGF. The main reason was the homogeneity of the C gel matrix. If the blended polymer does not have strong crosslinking characteristics like GT and XG under such conditions, creation of new interaction sites between the added polymer and continuous protein network could weaken the overall hydrogel matrix (Turgeon & Beaulieu, 2001). Addition of PC made the WPI hydrogels more susceptible to pepsin activity and low pH conditions due to the resulting structural inhomogeneity caused by PC degradation (Saldamli, 1998).

Besides different release profiles of hydrogels in SGF, hydrogels also possessed distinct release characteristics in SIF. Fig. 2 illustrates the percent increase in the release rates of samples with respect to their attained release rates right after 2 h SGF treatment. During 6 h SIF digestion, C hydrogels reached the highest increase in BC release percent as 31% ($p < 0.05$). XG, GT and PC hydrogels exerted lower increase in release rates as 21%, 19% and 15%, respectively ($p < 0.05$). Based on the results shown in Fig. 2, addition of polymer retarded BC release in SIF with pH around 6.8. The pH of the SIF was higher than both pI of the WPI and pKa values of the blended polymers so that polymers and protein molecules carried net negative charges. Under these conditions, indeed, chain relaxation mechanism due to excess charge repulsion would have been the dominant mechanism but the presence of KH_2PO_4 salt in SIF prevented this phenomenon (Argin, Kofinas, & Lo, 2014). Ionic strength of the SIF medium was 0.05 M and this created a charge screening effect diminishing the effect of electro-repulsive forces.

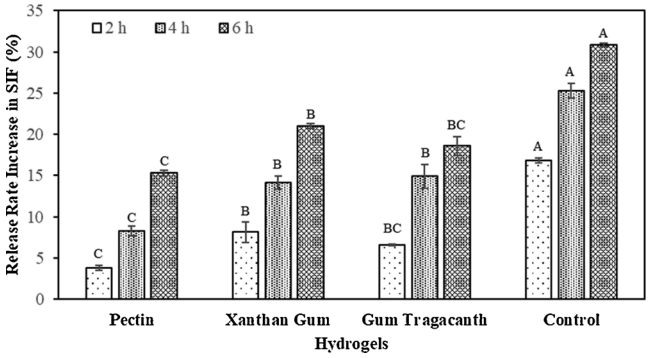

Fig. 2. BC release rate increase (%) of hydrogels during 6 h SIF digestion with respect to their attained release rates after SGF treatment ($p < 0.05$). Errors are represented as standard errors.

Crosslinking among the polymer chains is an important requirement for gelation and for the stability of the gels. In WPI hydrogels, crosslinking could occur due to disulfide linkages, electrostatic interactions, hydrophobic interactions and hydrogen bonding. In the case of a digestion medium and with the presences of polysaccharides electrostatic interactions are expected to contribute more. It was shown that in WPI hydrogels at alkaline pH, significant swelling was occurring due to strong charge repulsion among the polypeptide chains (Oztop, Rosenberg, Rosenberg, McCarthy, & McCarthy, 2010). Accordingly, at high pH conditions, charge repulsion would expect to loosen the gel network but at this ionic strength of the digestion medium, cations could have electrostatically interacted with the ionized groups and diminished their repulsive force. And the decreasing repulsive force could have enhanced the proximity between the molecules and crosslinking density could have increased via both hydrogen bonding and electrostatic attraction interactions (Jones & McClements, 2010). Accordingly, ions in the release medium enhanced the crosslinking within the hydrogel networks. Each hydrogel had different charge densities depending on the polymer used. Therefore, they possessed different crosslinking densities which affected their BC release behaviors in SIF. C samples having only WPI as the gelling agent, had lower charge density with respect to polymer added samples since at pH of 6.8, all added polymers contributed to abundance of the negatively charged portions of the gel networks. Consequently, C hydrogels experienced lower crosslinking within their molecular structure leading to higher BC release in SIF. PC, GT and XG molecules with highly negatively charged side groups, experienced more intense crosslinking and they retarded BC release in SIF. Clearly, charge screening effect was not the only factor influencing the release characteristics of the hydrogels in SIF. Hydrogen bonding interactions between the internal hydrogel polymer network surrounding the encapsulated agent and the anthocyanins of BC also played a crucial role in determining the release features of the hydrogels. Combination of WPI network with polymers created more interaction sites for BC anthocyanin molecules and the gel network, particularly via hydrogen bonding that retarded the BC release (Ferreira, Faria, Grosso, & Mercadante, 2009). Another factor was the presence of pancreatin enzyme in the SIF medium which caused degradation of the hydrogels. Pancreatic activity of the enzyme eroded hydrogels to some extent in SIF and the degree of erosion affected the release properties of the samples. Owing to the lower crosslinking density within the C hydrogels in SIF conditions, pancreatin enzyme could penetrate into the proteins of the C samples inducing plenty of structural defects by breaking hydrogen and disulfide bonds between protein molecules in the absence of any additional polymers and increased the BC release rate. Despite a lower crosslinking density due to its less branched molecular structure and lower charge density characteristic compared to XG molecules, PC hydrogels indicated a slower BC release profile in SIF as shown in Fig. 2 ($p < 0.05$). This condition was originally prompted by the fast release behavior of PC in SGF. Most of the bulk BC molecules located in the cavities within the PC hydrogel matrix were released in SGF. Remaining BC was slowly released in SIF, because rest of the BC was embedded in the depths of the gel matrix that was strongly interacting with the surrounding polymer reinforced protein network through hydrogen bonding. As a consequence, GT and XG blended samples possessing enhanced capacity to interact with BC molecules and high crosslinking degree within their gel network, could not retard BC release in SIF as much as PC hydrogels.

After the whole gastrointestinal digestion for 8 h, because of their rapid BC release in SGF, PC hydrogels attained the highest release rate (95%) ($p < 0.05$). On the other hand, C samples reached a higher cumulative release rate (88%) than XG and GT samples ($p < 0.05$) despite their similar retarded BC release profiles in SGF. The enhanced release behavior of C hydrogels in SIF led to this result. When the contributions of SGF and SIF release profiles to overall digestion were compared, it was obvious that all hydrogels achieved higher release rates in SGF than they did in SIF. There were two fundamental reasons for the observed trend relevant to the nature of the release media. Firstly, although SGF medium had an ionic strength of 0.034 M which was not much lower than the ionic strength of SIF (0.05 M), charge screening effect was much stronger in SIF medium. The strong acidic pH in SGF forced the carboxylic acid groups to remain in undissociated from and amino groups to be protonated residing in the hydrogels. For this reason, a whole positive charge distribution was expected within these hydrogels so that crosslinking throughout the hydrogels under SGF treatment was not as intense as in the case of SIF treatment (Wang, Chen, An, Chang, & Song, 2018). Secondarily, impacts of pepsin and pancreatin enzymes were different in terms of their proteolytic activity due to their distinct specifications. Characteristics of the β-Lg molecule regarding its susceptibility or resistance to aforementioned enzymes, even at partially unfolded form, also affected the digestibility of the hydrogels (Souza et al., 2012).

3.2. Protein loss from the hydrogels

Protein contents of the release media were determined in order to understand the effects of digestive enzymes on the composite WPI hydrogel structures and physicochemical interactions taking place within these hydrogels during digestion. As illustrated in Table 1, protein contents were considerably lower in SGF with respect to SIF medium. One of the reasons of the low protein loss of hydrogels in SGF was the resistance of native β-Lg to pepsin activity. Although β-Lg becomes susceptible to pepsin activity after unfolding by thermal denaturation, a small proportion of native β-Lg could still be observed even after heat induced denaturation treatment at 140 °C, 20 s and 80 °C, 30 min (Dissanayake, Ramchandran, Donkor, & Vasiljevic, 2013; Ju & Kilara, 1998). In our case, hydrogel solutions were subjected to heat treatment at 90 °C, 30 min, conforming this hypothesis. β-Lg conversion rate is accelerated with increase in pH (Hoffmann & Van Mil, 1997). At a critical pH around 7.5, β-Lg molecules undergo a conformational transformation known as *Tanford* transition during thermal denaturation (Tanford, Bunville, & Nozaki, 1959). By this new association, reactivity of thiol groups is increased and thiol-disulfide exchange

Table 1
Protein contents of the release media originating from the protein loss of respective hydrogels. Different letters in each column mean hydrogel type differed significantly ($p < 0.05$). Errors are represented as standard deviations.

Hydrogels	Protein Content in SGF 2 h (mg BSA/ ml)	Protein Content in SIF 8 h (mg BSA/ ml)
Control	1.40 ± 0.04^{c}	4.72 ± 0.06^{b}
Pectin	2.23 ± 0.05^{a}	4.91 ± 0.03^{b}
Gum Tragacanth	2.21 ± 0.03^{a}	5.31 ± 0.09^{a}
Xanthan Gum	1.73 ± 0.06^{b}	4.45 ± 0.16^{c}

reactions are enhanced. These reactions accelerate native β-Lg denaturation rate (Hoffman & Van Mil, 1999). Although both non-covalent (physical aggregation) and covalent interactions (thiol-disulfide exchange reactions) could contribute to the denaturation of native β-Lg at pH values also lower than 7.5, the final pH of the hydrogel solutions exposed to heat treatment were around 6.0, therefore thiol mediated reactions were not extremely enhanced in our case. These factors would lead to a slower native β-Lg denaturation rate, thus prompting presence of native β-Lg in our hydrogels. Other than the remnants of native β-Lg in hydrogels, strong acidic condition of SGF in which suppression of ionizable groups occurred also contributed to the low protein loss since the penetration of the pepsin enzyme was hindered by the compact nature of the hydrogels under these conditions. Unlike their counterparts releasing in SIF, hydrogels in SGF experienced shrinkage which protected their proteins from excess pepsin activity. Comparison of hydrogel types in SGF revealed that presence of polysaccharide in the WPI gel matrix could not reduce the protein loss of the hydrogels during SGF digestion (Table 1). This phenomenon indicated that intense interactions between proteins without any intervention by another polymer provided a better protection for proteins from getting hydrolyzed by pepsin in SGF. Yang et al. (2015) reported that addition of hsian-tsao gum to soy protein based films during film preparation (by heating at 80 °C, 30 min) weakened the interactions among the hydrophobic amino acid residues of soy protein isolate because of the presence of bulk hydrophilic part in hsian-tsao gum (Yang et al., 2015). High protein loss observed for the GT samples in SGF ($p < 0.05$) (2.21 mg BSA/ml in SGF medium) was also related to the decrease in reactions between proteins. GT is a physical mixture of water soluble and insoluble parts and the water soluble part including hydrophilic residues such as arabinogalactan imparts a strong liquid character to GT molecule (Balaghi et al., 2010). PC hydrogels shared the high protein loss feature with GT samples. PC hydrogels were the only ones that could not retard the BC release in SGF because of the weakening of the continuous WPI gel network. The high susceptibility of PC molecules to gastric conditions made it possible for pepsin enzyme to reach cleavage sites of the proteins. XG addition also reduced interactions between proteins and caused a relatively higher protein loss from XG hydrogels with respect to C hydrogels ($p < 0.05$). Under extreme acidic conditions where crosslinking between polymers and proteins were minimized, disulfide, hydrogen and hydrophobic interactions among protein molecules restrained pepsin activity. In the absence of any polymer that would otherwise constitute polymer-protein interactions and more protein unfolding, C hydrogels lost lower amount of protein from their matrixes in SGF ($p < 0.05$).

The higher protein content in SIF as indicated in Table 1, proved that pancreatic activity was more effective on hydrogels. Takagi et al. (2003) claimed that β-Lg was more labile in pancreatin containing SIF than pepsin containing SGF. After preheating (100 °C, 5 min) of β-Lg solution, β-Lg exerted stability in SGF, but it was easily digested in SIF (Takagi et al., 2003). In addition, *in vitro* digestibility studies of bovine milk whey protein demonstrated that β-Lg could be hydrolyzed by pancreatin both in native and heat denatured form (Kitabatake & Kinekawa, 1998). Pancreatin has a specific protein degradation activity mainly due to the presence of trypsin that is known to hydrolyze peptide bonds with distinct specificities. Trypsin action is focused on the peptide links involving the carboxylic groups of arginine and lysine (Beaulieu, Savoie, Paquin, & Subirade, 2002). Amino acid composition analysis of β-Lg revealed a considerably high proportion of lysine and arginine (Stein & Moore, 1949). Although all hydrogels experienced protein degradation in SIF, the most severe protein loss was observed in GT hydrogels ($p < 0.05$). As in the case of SGF treatment, hydrophilic character of GT helped pancreatin enzyme reach proteins interacting with GT polysaccharide in GT blended hydrogels during SIF treatment

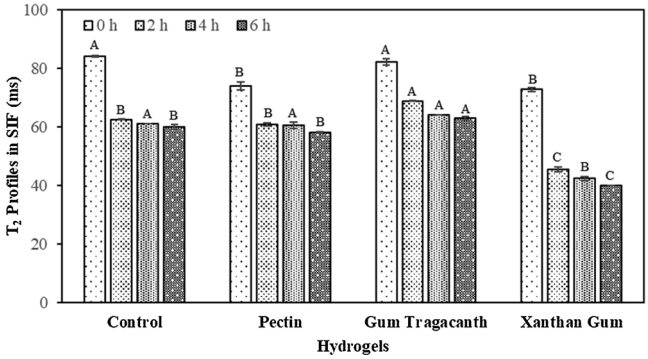

Fig. 3. T_2 profiles of hydrogels in SIF. 0 h represents the T_2 values of hydrogels after SGF treatment, 2–4 – 6 h represent digestion in SIF. Lettering is done for each time (0, 2, 4, 6 h, etc.) so that the hydrogels were compared for each time ($p < 0.05$). Errors are represented as standard errors.

and the outcome was the loss of more protein from these gel matrixes. XG addition retarded protein loss with respect to others in SIF ($p < 0.05$). Since the crosslinking mechanism was more pronounced in SIF, XG molecule contributed to denser polymer-protein interactions resulting in lower protein degradation within the hydrogels, quite opposite to the process occurred in SGF digestion. After SGF treatment, a glassy layer around XG hydrogels were observed. The helical structural conformation of XG molecule via interaction of its trisaccharide side chains with the cellulosic backbone in acidic condition induced such an observation (Saldamli, 1998). This rigid surface probably maintained its presence for some time in SIF treatment and reduced the penetration of pancreatin through the XG hydrogel. Protein loss values of C and PC samples in SIF were at intermediate levels. Under SIF conditions, C samples could not prevent protein degradation. Addition of PC also could not reduce the degraded protein level for PC hydrogels as in the case of XG hydrogels. Structural characteristics of PC molecule and its conformation in SIF conditions were the main reasons for this result.

3.3. NMR relaxometry

After 2 h SGF treatment, hydrogels attained T_2 values in the range of (73–84 ms) as shown in Fig. 3 (denoted by 0 h). T_2 values referred to the relaxation of water protons that are strongly associated with polymer network.

Undigested XG, C and PC hydrogels initially had similar T_2 values of 48, 49 and 50 ms, respectively. Untreated GT hydrogels with 54 ms initial T_2 had a longer T_2 than others before any treatment ($p < 0.05$). All hydrogels experienced longer T_2's after SGF treatment. PC hydrogels had shorter T_2 (74 ms) after SGF digestion due to their excess BC loss in SGF with respect to other SGF treated samples ($p < 0.05$). Although all transverse decays of hydrogels were monoexponential due to dominant effect of water – polymer interactions and fast exchange between different compartments, another important reason behind long T_2 could be the presence of BC in the hydrogels. Under these acidic conditions all gels experienced a shrinkage that obstructed the excess penetration of SGF medium into the depths of the samples. Retention of BC in the gel matrix increased the number of relaxing protons, in this way longer T_2 values were observed for C and GT hydrogels which retarded BC release in SGF ($p < 0.05$). XG samples also retarded the BC release in SGF but the enhanced interactions between the XG incorporated WPI hydrogel matrix and BC anthocyanins mainly via hydrogen bonding reduced the T_2 increasing effect of BC retention in XG hydrogels. Therefore, the state of encapsulated agent, which is BC in this case, in the gel matrix was also effective in T_2 determination

(Manetti, Casciani, & Pescosolido, 2004). Intense polymer-BC interactions in XG hydrogels gave rise to amount of BC molecules bound to surrounding polymer gel network. Amount of relaxing protons of bulk BC in free state was diminished (Ozel et al., 2018).

When SGF exposed hydrogels were placed in SIF for subsequent digestion (Fig. 3), T_2 values decreased and remained lower relative to their SGF correspondents throughout the SIF treatment ($p < 0.05$). The sudden reduction of T_2 could be explained by the nature of the SIF medium. Contrary to high hydrogen ion concentration in highly acidic condition of SGF that triggered longer spin-spin relaxation times, SIF has a pH of 6.8 and overall hydrogen ion concentration was lower in these conditions (Oztop et al., 2010). In addition to that, considerable amounts of BC in the hydrogels were lost in SGF so the lower BC content of hydrogels in SIF also paved the way for the lower T_2 profiles in that medium. On the other hand, protonated form of amino groups of proteins and carboxylic groups belonging to blended polysaccharides in SGF assisted the elevated T_2 trend of the SGF treated hydrogels. At the end of overall digestion, GT hydrogels attained the highest T_2 mainly related to its retarded release profile as well as the hydrophilic character of GT molecule that helped GT samples compensate the lost BC content with absorption of liquid release medium. The absorbed liquid also allowed pancreatic activity to increase by reaching interior protein cleavage sites within the GT hydrogel. Nevertheless, XG samples having also a retarded BC release profile in SIF, had the lowest T_2 values. This T_2 pattern clearly showed that the lost amount of BC could not be equilibrated by the absorption of liquid medium into the XG hydrogels. Highly cross-linked gel network and relatively harder outer surface of the XG hydrogels did not permit adequate SIF penetration into the interiors of the gel network resulting in lower T_2 values after the digestion. Although C hydrogels attained the fastest BC release rate in SIF, they apparently compensated this loss by absorbing a certain amount of release medium that balanced the amount of liquid residing within the hydrogel. Penetration of liquid release medium into the C hydrogels was eased by the low crosslinking density within the C samples due to the absence of an additional polymer that would intensify the cross-linking throughout the WPI gel network under SIF conditions. Therefore, T_2 of C hydrogels did not undergo a severe decrease during release in SIF contrary to XG blended samples. Because of the limited BC release of PC hydrogels and the absorption of some surrounding liquid into the gel network in SIF, T_2 of PC hydrogels remained at an intermediate level between GT and XG hydrogels.

Another element that would be used to comprehend the release behaviors of hydrogels in gastrointestinal conditions was the percent crystallinity content measurements by NMR relaxometry (Maus, Hertlein, & Saalwächter, 2006). Results were shown in Table 2 and it was observed that addition of polymer increased the crystalline fraction of the hydrogels that were not exposed to any release media (0 h) except for GT blended hydrogels ($p < 0.05$). Creation of new interaction sites via more physical interactions between the continuous WPI network and the blended PC and XG molecules decreased the amorphous character of only WPI containing C samples. The high hydrophilic feature of GT contributing to the weak gel character of GT hydrogels, could not sufficiently change the amorphous fraction dominating the protein gel network. Gastric treatment increased the amorphous contribution in PC and XG hydrogel microstructures initially having higher crystallinity percentages ($p < 0.05$). When exposed to liquid media, polymer-water interactions caused a smoother texture within the PC and XG hydrogels so that the percent crystallinity contents decreased ($p < 0.05$) (Ozel et al., 2017). SIF exposure following the SGF treatment did not affect the fractions of the crystalline and amorphous regions of any hydrogels. Rather than the morphological changes within depths of the hydrogels, erosion of the gel matrixes occurring mainly on the gel surfaces took place in SIF conditions and all hydrogels followed a stable profile in terms of percent crystallinity contents. Release rates of PC and XG hydrogels were found highly inversely correlated in Pearson correlations ($r > 0.94$ for PC, $r > 0.97$ for XG) in the whole (8 h) digestion. Therefore, digestion increased the amorphous character of hydrogels having relatively higher crystalline fractions in the beginning. Especially C hydrogels did not undergo a significant difference in their crystalline and amorphous structures throughout the whole digestion proving the effect of polysaccharide addition on the crystallinity of the hydrogels.

3.4. FTIR spectra of hydrogels

FTIR analyses were performed for the freeze-dried powder form of hydrogels after 2 h SGF treatment and 8 h complete digestion (SGF + SIF) as shown in Fig. 4a–d. Generally, absorption bands of SIF treated samples that were initially subjected to SGF, showed increase with respect to the bands obtained after only SGF treatment. A couple of new absorption peaks were also detected for the hydrogels after SIF treatment. Despite some similar patterns and identical positions of the peaks at specific wavenumbers, each hydrogel possessed distinct absorption band features at these wavenumbers. Firstly, the characteristic peak detected at 1633 cm^{-1} is called as amide I band and it is related to the C=O stretching of the protein backbone (Bandekar, 1992). This band determines the nature of hydrogen bonds involving in C=O and N−H groups of the peptide linkages. Amide I region is sensitive to conformational changes in the secondary structure of proteins indicating mainly the intermolecular hydrogen bonded β-sheet structures of aggregated proteins (Lefèvre & Subirade, 1999). Hydrogen bond strength and the geometry of the secondary structures also have impacts on amide I band. Another peak located at 1519 cm^{-1} represents the N−H and C−N vibrations in peptide bonds and it is known as amide II band (Xu & Dumont, 2015). Peaks between 1200 and 1400 cm^{-1} belonging to amide III bands also responsible for the vibrations of N−H and C−N groups (Díaz, Candia, & Cobos, 2016). Vibrations in the $-CH_2$ groups of glycine also contributes to the band intensity in this range (Aewsiri, Benjakul, & Visessanguan, 2009). The broad peak between 3000 – 3500 cm^{-1} having a maximum absorbance point at 3275 cm^{-1} demonstrates the hydroxyl group vibrations involving the stretching of the total free and bonded O−H and N−H groups (Ebrahimi et al., 2016). 2960 and 3064 cm^{-1} peaks are attributed to symmetric and asymmetric −CH stretching, respectively. $-NH_2$ stretching vibrations as well as $-CH_2$ and $-CH_3$ groups stretching can also be referred to these peaks (Mostafavi et al., 2016). Another peak located at 1068 cm^{-1} originates from the C−O stretching (Ebrahimi et al., 2016). This peak could be originated from sugar glycosidic bond and C−O – C in the sugar ring.

Table 2
Percent crystallinity values of hydrogels: (0 h) untreated, (2 h) only SGF treated, (8 h) SIF digested hydrogels after SGF treatment. Different small letters show that hydrogel types differed significantly, in each column ($p < 0.05$). Different capital letters show that implementation or type of digestion media affected the crystallinity values significantly, in each row ($p < 0.05$). Errors are represented as standard deviations.

Hydrogels	Crystallinity 0 h (%)	Crystallinity 2 h (%)	Crystallinity 8 h (%)
Control	$23.92 \pm 0.43^{b, A}$	$22.72 \pm 1.13^{b, A}$	$22.09 \pm 0.98^{b, A}$
Pectin	$30.18 \pm 1.71^{a, A}$	$22.68 \pm 0.15^{b, B}$	$22.42 \pm 0.72^{b, B}$
Gum Tragacanth	$23.24 \pm 0.88^{b, B}$	$26.33 \pm 0.60^{a, A}$	$24.73 \pm 0.98^{ab, AB}$
Xanthan Gum	$30.19 \pm 0.62^{a, A}$	$26.38 \pm 0.50^{a, B}$	$25.66 \pm 0.93^{a, B}$

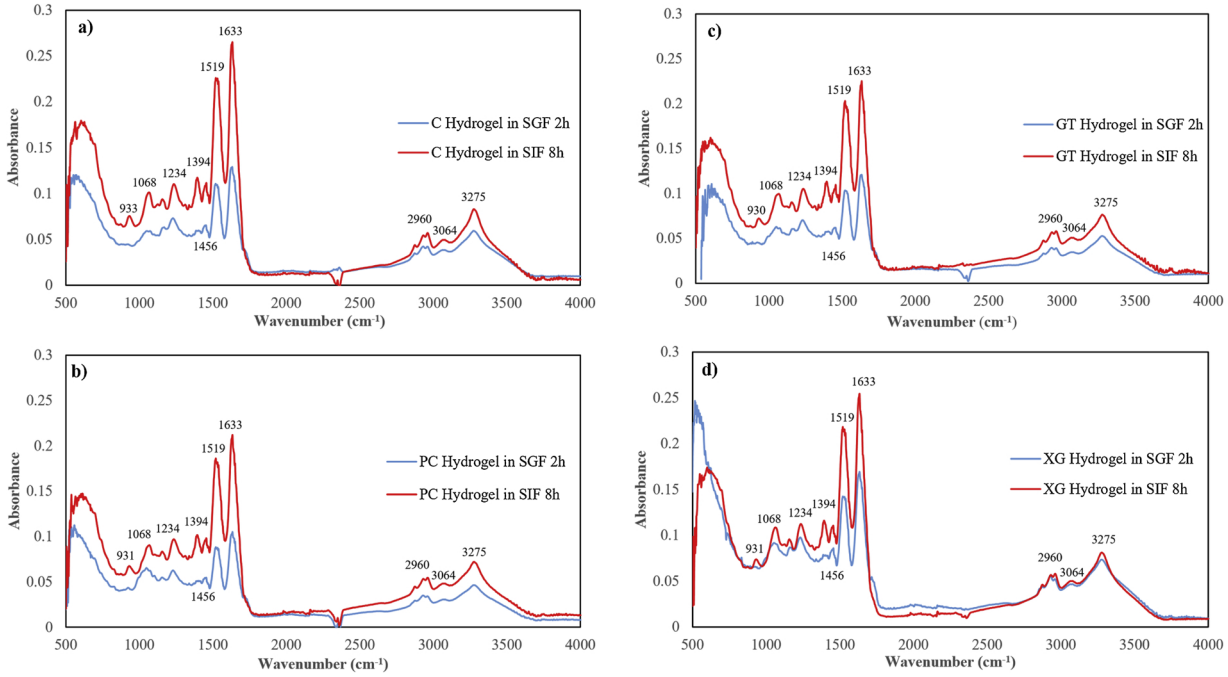

Fig. 4. FTIR spectra of only SGF treated hydrogels (Hydrogel in SGF 2 h) and SIF digested hydrogels after SGF treatment (Hydrogel in SIF 8 h): (a) Control, (b) Pectin, (c) Gum Tragacanth, (d) Xanthan Gum.

Besides, the peak could be associated with the presence of carboxylic acid units implying the polysaccharides existence. Galacturonic acid, glucose, galactan and arabinogalactan residues may contribute to the absorbance intensity of this band. Symmetrical −COO stretching were observed at 1456 cm^{-1} for both SGF and SIF treated samples (Cai et al., 2010).

FTIR spectra of polysaccharide powders and freeze-dried untreated hydrogels were also obtained (see supplementary file). Spectrum of WPI showed differences in terms of band peak positions and spectral densities with respect to spectra of polysaccharides. Amide I intensity of WPI was quite higher due to presence of protein. There was no such a peak in polysaccharides as expected. In contrast, polysaccharides possessed a peak around 1040 cm^{-1} proving the presence of carboxylic acid units specific to polysaccharides. WPI powders did not show any peak at that wavenumber. All untreated hydrogels attained higher peak intensities than their polysaccharide powder form correspondents. Lower intensity of hydroxyl group stretching in XG hydrogels was related to the intense interactions between XG molecules and WPI. This peak enhanced due to solvent introduction to polysaccharide and WPI powders and all other hydrogels attained higher O−H vibration intensities indicating a higher level of polymer – water interactions. Rigid form of XG in solutions prevented better hydration of the molecule.

SIF digestion following 2 h SGF treatment caused an increase in the amide band intensities of all hydrogels indicating the effect of pancreatic activity during SIF treatment (Fig. 4a–d). The spectral intensity increase in the amide I regions was related to the final structure of proteins in freeze-dried hydrogels. Changes in the secondary structure geometry of the proteins were induced by the increase in the structural mobility of the proteins during digestion and these changes were also prompted by the degradation of protein parts of the hydrogels. Under SIF conditions, peptide N−H protons present in the unfolded polypeptides exchanged with the aqueous solvent via hydrogen bonding that increased protein dissolution (Dong et al., 1996). These factors increased the vibrations of amide I band. The higher amide I spectral intensity was also the result of the increased number of free amino groups formed due to the hydrolysis of the peptide linkages (Su, Huang, Yuan, Wang, & Li, 2010). Other factors that would contribute to the higher amide I intensity were the amount of protein and the effect of heating. Shape of the peak at 1633 cm^{-1} representing the complete protein aggregation is also important in terms of secondary structure characteristics since a smooth peak in amide I region means a more disordered secondary structure. Lefèvre and Subirade (1999) reported that heating of β-Lg solutions (1–10% w/w) at 85 °C broadened the amide I peak located between 1600 and 1700 cm^{-1} by eliminating the other peaks arose in that region. Effect of heating was promoted by longer heating times. Amide I band of SIF treated hydrogels showed this broadened feature with one distinct peak in amide I region (1633 cm^{-1}) and the spectral increase of this peak after the SIF digestion suggested a more disordered secondary structure for all hydrogels (Fig. 4a–d) (Lefèvre & Subirade, 1999). Increase in the spectral intensities of amide II and amide III regions were also driven by the hydrolysis of peptide bonds. N−H and C−N vibrations at 1519 cm^{-1} were enhanced with higher hydrogen bonding between these groups and the aqueous media. Similar effect of proteolysis was also observed for amide III region. An additional peak around 1394 cm^{-1} appeared after SIF digestion for all hydrogels (Fig. 4a–d). The increase in the free state vibrations of N−H and C−N groups after the breaking of long polypeptide chains probably created this peak. Another peak that was observed only after SIF treatment was the peak between 930 and 933 cm^{-1} again for all hydrogels. Skeleton C−C vibrations were responsible for these peaks (Ebrahimi et al., 2016). The intensity of C−C stretching located in the long protein molecules were not high enough to reveal a peak in that region but breaking of peptide bonds after SIF digestion enabled C−C groups to vibrate freely leading to another peak in amide III region.

A rising trend for the O−H spectral intensities at 3275 cm^{-1} was observed after exposure to SIF for all freeze-dried samples expect for XG hydrogels. Formation of intermolecular hydrogen bonding with the carbonyl groups of peptide linkages was effective in the enhancement of this band. Retention of BC in the hydrogels and the level of bound water present in the hydrogels after freeze-drying process were the other determinant factors that altered the intensity and shape of the O−H bands. Slight increases in O−H spectral intensities of C, PC and GT hydrogels (Fig. 4a–c) suggested that these hydrogels formed more

hydrogen bonding with the surrounding aqueous medium during digestion since correspondent amount of strongly bound water increased for these hydrogels as determined by the FTIR spectroscopy measurements. Contribution of free −OH and –NH groups could also be higher for these samples with respect to XG hydrogels. Dissolution of proteins from GT, PC and C samples were higher than XG hydrogels in SIF, proving that claim ($p < 0.05$). Apart from their higher absorbance values in O−H region, C, PC and GT hydrogels also possessed wider peaks compared to XG hydrogels. Broadened O−H peaks of these hydrogels emerged from the increase in the number of −OH groups involved in hydrogen bonding with respect to free −OH groups (Fattahi et al., 2013). The reason of this phenomenon was the higher ionization of the ionizable groups residing in C, PC and GT gel networks under SIF conditions. On the other hand, intense interactions between XG molecule and WPI in SIF resulted in lower amounts of ionization throughout the gel matrix. Although C samples lost the highest amount of BC during SIF treatment ($p < 0.05$), they experienced a mild increase in the peak located at 3275 cm^{-1} (Fig. 4a). BC loss from the gel matrix would decrease the hydrogen bonding interactions but clearly hydrogen bonding intensity with the aqueous media was high for these hydrogels leading to a high level of final bound water and protein dissolution overcome the BC loss effect. GT samples experienced a lower BC release compared to C samples in SIF ($p < 0.05$). In addition, the high protein loss from GT gel matrix and noteworthy hydrogen bonding interactions with the surrounding liquid in the exchange for BC release during SIF treatment, contributed to the extent of hydroxyl group interactions. The slow BC release behavior of PC hydrogels combined with the protein degradation readily ensured the spectral intensity increase in the peak at 3275 cm^{-1} (Fig. 4b). Stability of the O−H band of XG hydrogels after SIF treatment was mainly due to the low protein loss from XG blended hydrogel matrix (Fig. 4d). This reduced the hydrogen bond and free −OH group formations in XG samples. Although XG hydrogels retarded BC release in SIF compared to C hydrogels ($p < 0.05$), interactions with encapsulated BC molecules were not sufficient to increase the O−H band intensity. Moreover, low amount of liquid intake from release medium also among the factors that provided a stable O−H stretching band after whole digestion of XG samples since this low amount of water was not sufficient to fully hydrate the complex structure of XG hydrogels. Treatments before FTIR spectroscopy measurements removed this absorbed water fraction, excessively. Other FTIR spectra differences between XG and rest of the hydrogels were in the amide regions. Despite the considerable absorbance increase observed in the amide regions of C, PC and GT samples, subtle absorbance increase of the amide bands especially in amide II and III regions of XG hydrogels verified the intense interactions between XG molecules and the protein network that decreased the hydrolysis of the peptide linkages between proteins.

Absorbance values of symmetric −CH stretching peak at 2960 cm^{-1} increased after SIF treatment for all hydrogels expect for XG containing hydrogels (Fig. 4a–d). The increase of this peak demonstrated that the degree of disordered hydrocarbon chains was boosted (Kodati & Lafleur, 1993). Dissolution of proteins taking place during SIF treatment increased the hydration of polar groups and responsible peaks at 2960 and 3064 cm^{-1} were enhanced for C, PC and GT hydrogels (Fig. 4a–c). Stable peak characteristics of XG hydrogels in these bands were also coherent with the limited protein degradation characteristics of XG hydrogels during SIF digestion.

3.5. Texture profiles

Hardness values of hydrogels were demonstrated in Fig. 5. Before digestion, XG hydrogels had the lowest hardness value (1.97 N) with respect to other hydrogels ($p < 0.05$). Polymer added hydrogels attained softer structures in the absence of any external stimuli. C samples having initial hardness of 7.27 N, apparently provided a homogeneity in terms of molecular interactions throughout the gel matrix (Yang et al., 2015). However, when exposed to gastrointestinal fluids, polymers contributed differently to the gel strengths due to their different physicochemical responses in the release media induced by their distinct molecular characteristics. SGF treatment softened all hydrogels expect for XG hydrogels ($p < 0.05$). High molecular charge density and rigid conformation of its main backbone under acidic conditions intensified the interactions between XG and WPI molecules (Zhang et al., 2014). Weaker gel structures of PC and GT hydrogels, on the other hand, were in agreement with the previous literature findings (Fattahi et al., 2013; Ozel et al., 2018). Hardness values of all hydrogels increased after subsequent SIF digestion (Fig. 5). This was an expected phenomenon because of the ionic nature of SIF which made crosslinking interactions possible in contrast to SGF medium (Jones & McClements, 2010). Even higher protein degradation in SIF could not withhold the hardening of the hydrogels in SIF. At the end of 8 h simulated gastrointestinal digestion, XG hydrogels had the highest gel hardness as 8.73 N ($p < 0.05$). PC blended hydrogels obtained a hardness value of 2.19 N after 8 h which was the lowest level among the others ($p < 0.05$). When compared with their cumulative release rates (8 h), XG hydrogels attained the lowest release rate (73.43%) and PC samples attained the highest release rate around 95% so that it was obvious that higher gel strength retarded the BC release in gastrointestinal digestion ($p < 0.05$). XG gels also followed a different hardness trend with respect to other gels. Hardness of XG samples increased continuously in gastrointestinal conditions whereas all other samples experienced weaker gel structures after SGF treatment. These hardness results mainly originated from the abundance of crosslinkings between XG blended protein gel network particularly in SIF conditions. Increasing hardness trend of XG hydrogels were also supported by the lowest T_2 values, stable −OH band characteristics, lowest protein loss during SIF treatment and the highest crystallinity percentage of these hydrogels after 8 h complete

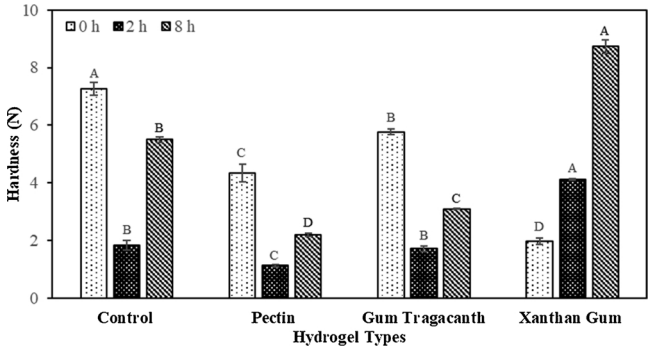

Fig. 5. Hardness profiles of hydrogels: (0 h) untreated, (2 h) only SGF treated, (8 h) SIF digested hydrogels after SGF treatment. Lettering is done for each time (0, 2 and 8 h) so that the hydrogels were compared for each time ($p < 0.05$). Errors are represented as standard errors.

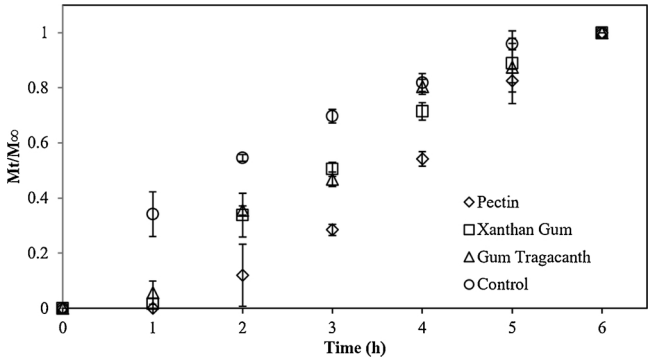

Fig. 6. Release trend of hydrogels in SIF. Errors are represented as standard errors.

digestion ($p < 0.05$).

3.6. Release trend in SIF

Release trends of hydrogels during 6 h release in SIF were estimated as shown in Fig. 6. Previously, all hydrogels were treated in SGF for 2 h. Understanding the release trends, thus the release mechanisms of controlled release systems, is crucial in terms of optimization of the release phenomenon. Release mechanisms of protein-based delivery systems depend on the nature and amount of encapsulated bioactive agent, protein composition, composition and type of any other blended polymer, release media and the geometry of the delivery tool. Four mechanisms, mainly diffusion, erosion, swelling-shrinkage and fragmentation govern the release phenomena (Fathi et al., 2018). SIF release data could not be identified by power law or any other model because of the irregular release behaviors of the hydrogels during SIF digestion. Additionally, substantial reductions in the hydrogel dimensions were detected after digestion was completed. Therefore it was concluded that, BC release was driven mainly by enzymatic erosion in SIF having pancreatin as the digestive enzyme in contrast to diffusion controlled release in SGF conditions (Ozel et al., 2018). Chen and Subirade (2006) have also indicated that the driving force for riboflavin release from alginate-whey protein granular microspheres in pancreatin containing SIF was the erosion of the microspheres and a fitting release model could not be identified for this process (Chen & Subirade, 2006). Because of the gradual size reduction of the hydrogels in SIF, they experienced a heterogeneous erosion which took place mainly at the hydrogel surface. In contrast to heterogeneous erosion, homogeneous erosion (also known as bulk erosion) would not induce a size reduction of the gel and the size of the gel would remain constant. In this case, external fluid would penetrate into the system by breaking the chemical and physical bonds so that erosion would take place in the bulk volume of the hydrogel (Zhang, Yang, Chow, & Wang, 2003). However, because of the size reduction, SIF treated hydrogels eroded at the external boundary and this led to surface erosion of the hydrogels. High protein degradation results of SIF treated hydrogels were compatible with this erosion model.

When Fig. 6 was examined, it was detected that within the first hour of the SIF digestion, hydrogels could not release a considerable amount of BC except for C hydrogels. Primary reason for this behavior was the dominant effect of charge screening that eliminated the charge repulsion within the hydrogels in the beginning of the SIF digestion. With a lower charge density, C hydrogels experienced a more charge repulsion with respect to polymer added samples that had increased crosslinking within their structures. Nevertheless, starting from around 2 h, erosion of hydrogels by pancreatic activity dominated the release behaviors. Due to the substantial increase in the hydrogel matrix degradations, hydrogels experienced a burst release in SIF (Wang et al., 2018). Direct contact of pancreatin enzyme with proteins on the hydrogel surfaces dramatically changed the initial release trends of the hydrogels in SIF (Xu & Dumont, 2015).

3.7. Weight loss of hydrogels in SIF

Hydrogels exhibited a considerable amount of matrix weight loss during SIF treatment due to erosion that mainly occurred on their surfaces (Table 3). Although XG hydrogels experienced the lowest protein loss from their gel matrixes, they possessed the most severe weight loss (43.63%) with respect to other samples ($p < 0.05$). Therefore, identifying sort of the weight loss is quite important. Contrary to XG hydrogels, GT samples lost the highest amount of protein from their gel matrixes in SIF ($p < 0.05$). However, GT hydrogels did not lose as much weight as XG hydrogels in SIF, even they shared the lowest weight loss values with C samples, 32% and 33.3%, respectively ($p < 0.05$). Since XG and GT hydrogels attained similar BC release rate increase percentages after SIF treatment, the dramatic difference between their weight loss values was driven by their distinct interactions with the surrounding release medium. The highest T_2 of GT and the lowest T_2 of XG hydrogels showed that GT samples compensated their weight loss by absorption of liquid from the surrounding liquid medium whereas XG samples could not absorb as much liquid medium as GT samples. This phenomenon was also substantiated by FTIR results since the O—H band of XG hydrogels was rather stable while the others had broadened and slightly higher peaks after SIF digestion. This proved the rare hydroxyl group vibrations taking place within the XG samples due to the presence of lower amounts of liquid in the XG hydrogels (Ebrahimi et al., 2016). PC hydrogels having intermediate protein loss in SIF, also attained intermediate weight loss as demonstrated in Table 3. Despite high amount of BC release in SIF, the low weight loss of C samples was related to high absorption of release medium which was also proven by T_2 and FTIR measurements.

Table 3
Weight loss results of hydrogels in SIF treatment ($p < 0.05$). Errors are represented as standard deviations.

Hydrogels	Weight Loss in SIF (%)
Control	33.30 ± 1.79^{c}
Pectin	38.74 ± 1.47^{b}
Gum Tragacanth	32.00 ± 1.12^{c}
Xanthan Gum	43.63 ± 1.42^{a}

3.8. Microstructures of hydrogels

SEM images (Fig. 7) showed the morphological changes in the hydrogel microstructures induced by polymer addition and the type of the exposed release medium. SGF treatment revealed structurally integrated continuous matrices for all hydrogels. Different physiochemical changes of hydrogels due to SGF treatment affected the intensity of the interactions, thus the distribution of the aggregates formed within the hydrogels. Only SGF treated C hydrogels possessed relatively big and hexahedral shaped aggregates (Fig. 7a). Formation of these distinct coarse particles on the closely packed smooth surface was attributed to sucrose crystals interacting with whey protein particles since encapsulated BC has a considerable sugar content including sucrose with the highest proportion (Harnkarnsujarit & Charoenrein, 2011; Ozel et al., 2018). In several studies, it was reported that, whey proteins could act as nuclei, promoting primary heterogeneous nucleation of lactose (Sánchez-García, Gutiérrez-Méndez, Orozco-Mena, Ramos-Sánchez, & Leal-Ramos, 2019). Moreover, Pérez, Piccirilli, Delorenzi, and Verdini (2016) stated the presence of rhombohedral crystals of trehalose on the whey protein film surfaces (Pérez et al., 2016). Despite their smaller size, intensity of these hexahedral aggregates was higher in only SGF treated GT hydrogels (Fig. 7e). XG hydrogels had even smaller sized aggregates with greater intensity after 2 h exposure to SGF (Fig. 7g). XG samples were also the hardest gels after SGF treatment ($p < 0.05$). Only SGF digested PC hydrogels, exerted a heterogeneous and less dense distribution of big coarse particles having more irregular orientations (Fig. 7c). The weakest gel strength of PC hydrogels after SGF exposure was in agreement with microstructural observations. When percent crystallinity results of hydrogels were compared with SEM images, it was observed that more homogeneous distribution of aggregates having smaller sizes led to higher percent crystallinity values since XG and GT hydrogels attained higher crystal fractions at the end of 2 h gastric digestion ($p < 0.05$). Implementation of SIF after SGF treatment created smoother clumpy structures for all hydrogels because of the enhanced entanglement and intermolecular interactions between the polymers and WPI molecules (Fig. 7). C hydrogels attained a milder network with prominent surface defects in the absence of an additional polymer (Fig. 7b). Presence of more distinct aggregates in polymer added and SIF treated hydrogel microstructures (PC, GT and

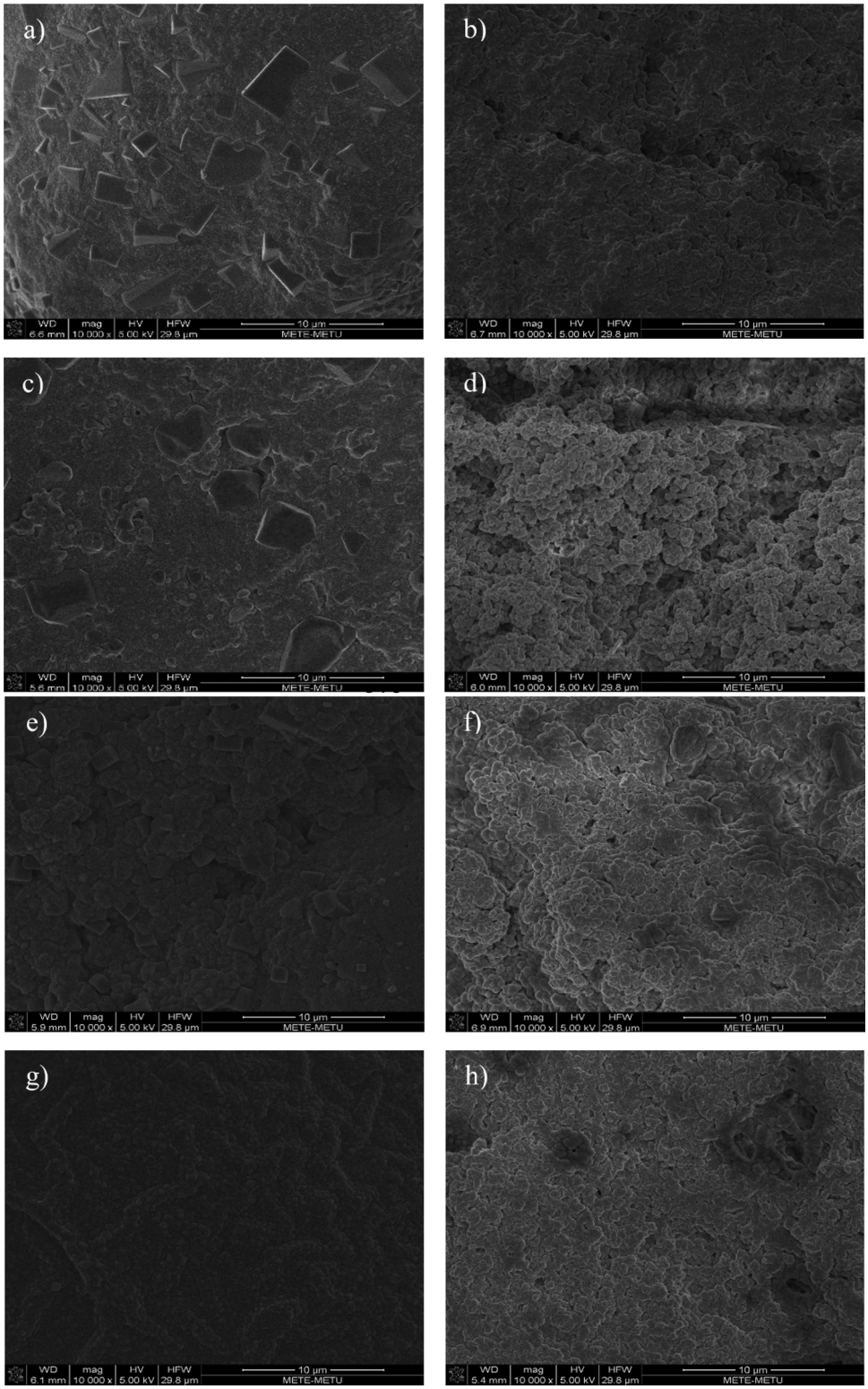

Fig. 7. SEM images of only SGF treated hydrogels and SIF digested hydrogels after SGF treatment: (a) only SGF treated C, (b) SGF + SIF treated C, (c) only SGF treated PC, (d) SGF + SIF treated PC, (e) only SGF treated GT, (f) SGF + SIF treated GT, (g) only SGF treated XG, (h) SGF + SIF treated XG hydrogels.

XG) manifests the impact of polymer blending to hydrogels in SIF conditions. Apart from these, pancreatic activity promoted some cavities and cracks producing discontinuities within the SIF treated gel networks which was an indicator of protein loss from the matrixes. Size distribution of crystal aggregates were narrowed by whey protein molecules in SIF as a result of the alteration in the pH (Sánchez-García et al., 2019). Consequently, crystal fractions of hydrogels did not change significantly during SIF treatment ($p < 0.05$). Despite the structural changes, hardening of the hydrogels in SIF indicated that the surface erosion character of digestion in SIF helped hydrogels maintain a relatively stable amorphous/crystal fraction.

4. Conclusions

BC loaded composite WPI hydrogels were developed for in vitro release in gastrointestinal conditions. Created gel matrixes provided prolonged release profiles for the hydrogels both in SGF and SIF. Since BC anthocyanins are especially unstable in SIF conditions having a pH at 6.8, achievement of slow release in this medium was crucial. Addition of polymers induced different physicochemical interactions within the hydrogels and these interactions were analyzed mainly by NMR relaxometry, FTIR spectroscopy and protein solubility measurements. Moreover, texture measurements and SEM images contributed to the characterization of the physicochemical changes taking place in the hydrogels. Distinct features of the release media played the major role in the release profiles. All hydrogels remained intact in SGF while C, GT and XG hydrogels had retarded release profiles with respect to PC hydrogels ($p < 0.05$). Hydrogels were fairly protected from pepsin activity. After 2 h SGF treatment, 6 h SIF digestion revealed that polymer blending retarded the release rates ($p < 0.05$). Different composition, enzyme and pH environment of SIF changed the release behaviors of hydrogels which they previously experienced in SGF. Although hydrogels were subjected to a gradual protein degradation by surface erosion causing a decrease in dimensions in SIF conditions, they remained their solid characteristics until the end of the digestion. This assured a gradual and continual BC release in SIF which could be used as a prototype for in vivo intestinal digestion. The study showed that hydrogels would reach the upper intestine undigested and considerable amounts of hydrogels would also reach the final section of the small intestine in undigested form. Results also indicated that addition of polymer to WPI hydrogels provided appropriate release characteristics during intestinal digestion. With its moderate hardness throughout the digestion and gradual release in SIF, GT hydrogels offer a desirable BC delivery. These attributes of hydrogels could be employed for in vivo models that aim to increase satiety and trigger prolonged residency of the active agent in the small intestine.

Acknowledgments

We would like to thank Ulku Ertugrul and Berkay Bolat for their contribution to the study. We also would like to acknowledge COST Action CA 15209 EURELAX - European Network on NMR Relaxometry since some of the findings were discussed in the action's network meetings. A part of the funding also came from Dr. Oztop's award of Science Academy's Young Scientist Awards Program (BAGEP) and Middle East Technical University research funds with grant # DKT-314-2018-3596.

Appendix A. Supplementary data

Supplementary material related to this article can be found, in the online version, at doi:https://doi.org/10.1016/j.carbpol.2019.115469.

References

Aewsiri, T., Benjakul, S., & Visessanguan, W. (2009). Functional properties of gelatin from cuttlefish (Sepia pharaonis) skin as affected by bleaching using hydrogen peroxide. *Food Chemistry, 115*(1), 243–249. https://doi.org/10.1016/j.foodchem.2008.12.012.

Akhtar, S., Rauf, A., Imran, M., Qamar, M., Riaz, M., & Mubarak, M. S. (2017). Black carrot (Daucus carota L.), dietary and health promoting perspectives of its polyphenols: A review. *Trends in Food Science & Technology, 66*, 36–47. https://doi.org/10.1016/j.tifs.2017.05.004.

Arab, F., Alemzadeh, I., & Maghsoudi, V. (2011). Determination of antioxidant component and activity of rice bran extract. *Scientia Iranica, 18*(6), 1402–1406. https://doi.org/10.1016/j.scient.2011.09.014.

Argin, S., Kofinas, P., & Lo, Y. M. (2014). The cell release kinetics and the swelling behavior of physically crosslinked xanthan-chitosan hydrogels in simulated gastrointestinal conditions. *Food Hydrocolloids, 40*, 138–144. https://doi.org/10.1016/j.foodhyd.2014.02.018.

Arts, I. C. W., & Hollman, P. C. H. (2005). Polyphenols and disease risk in epidemiologic studies 1–4. *The American Journal of Clinical Nutrition, 81*, 317–325.

Balaghi, S., Mohammadifar, M. A., & Zargaraan, A. (2010). Physicochemical and rheological characterization of gum tragacanth exudates from six species of Iranian Astragalus. *Food Biophysics, 5*(1), 59–71. https://doi.org/10.1007/s11483-009-9144-5.

Balaghi, S., Mohammadifar, M. A., Zargaraan, A., Gavlighi, H. A., & Mohammadi, M. (2011). Compositional analysis and rheological characterization of gum tragacanth exudates from six species of Iranian Astragalus. *Food Hydrocolloids, 25*(7), 1775–1784. https://doi.org/10.1016/j.foodhyd.2011.04.003.

Bandekar, J. (1992). Amide modes and protein conformation. *Biochemica et Biophysica Acta, 1120*(2), 123–143. https://doi.org/10.1016/0167-4838(92)90261-B.

Bateman, L., Ye, A., & Singh, H. (2011). Re-formation of fibrils from hydrolysates of β-lactoglobulin fibrils during in vitro gastric digestion. *Journal of Agricultural and Food Chemistry, 59*(17), 9605–9611. https://doi.org/10.1021/jf2020057.

Beaulieu, L., Savoie, L., Paquin, P., & Subirade, M. (2002). Elaboration and characterization of whey protein beads by an emulsification/cold gelation process: Application for the protection of retinol. *Biomacromolecules, 3*(2), 239–248. https://doi.org/10.1021/bm010082z.

Belscak-Cvitanovic, A., Komes, D., Karlović, S., Djaković, S., Špoljarić, I., Mršić, G., ... Ježek, D. (2015). Improving the controlled delivery formulations of caffeine in alginate hydrogel beads combined with pectin, carrageenan, chitosan and psyllium. *Food Chemistry, 167*, 378–386. https://doi.org/10.1016/j.foodchem.2014.07.011.

Betz, M., & Kulozik, U. (2011). Whey protein gels for the entrapment of bioactive anthocyanins from bilberry extract. *International Dairy Journal, 21*(9), 703–710. https://doi.org/10.1016/j.idairyj.2011.04.003.

Biehler, E., & Bohn, T. (2010). Methods for assessing aspects of carotenoid bioavailability. *Current Nutrition and Food Science, 6*(1), 44–69. https://doi.org/10.2174/157340110790909545.

Bouayed, J., Hoffmann, L., & Bohn, T. (2011). Total phenolics, flavonoids, anthocyanins and antioxidant activity following simulated gastro-intestinal digestion and dialysis of apple varieties: Bioaccessibility and potential uptake. *Food Chemistry, 128*(1), 14–21. https://doi.org/10.1016/j.foodchem.2011.02.052.

Cai, J., Yang, J., Wang, C., Hu, Y., Lin, J., & Fan, L. (2010). Structural characterization and antimicrobial activity of chitosan (CS-40)/nisin complexes. *Journal of Applied Polymer Science, 116*, 3702–3707. https://doi.org/10.1002/app.31936.

Chen, L., & Subirade, M. (2006). Alginate-whey protein granular microspheres as oral delivery vehicles for bioactive compounds. *Biomaterials, 27*(26), 4646–4654. https://doi.org/10.1016/j.biomaterials.2006.04.037.

Dag, D., Kilercioglu, M., & Oztop, M. H. (2017). Physical and chemical characteristics of encapsulated goldenberry (Physalis peruviana L.) juice powder. *LWT – Food Science and Technology, 83*, 86–94. https://doi.org/10.1016/j.lwt.2017.05.007.

De la Fuente, M. A., Singh, H., & Hemar, Y. (2002). Recent advances in the characterisation of heat-induced aggregates and intermediates of whey proteins. *Trends in Food Science & Technology, 13*(8), 262–274. https://doi.org/10.1016/S0924-2244(02)00133-4.

Díaz, O., Candia, D., & Cobos, Á. (2016). Effects of ultraviolet radiation on properties of films from whey protein concentrate treated before or after film formation. *Food Hydrocolloids, 55*, 189–199. https://doi.org/10.1016/j.foodhyd.2015.11.019.

Dissanayake, M., Ramchandran, L., Donkor, O. N., & Vasiljevic, T. (2013). Denaturation of whey proteins as a function of heat, pH and protein concentration. *International Dairy Journal, 31*(2), 93–99. https://doi.org/10.1016/j.idairyj.2013.02.002.

Dong, A., Matsuura, J., Allison, S. D., Chrisman, E., Manning, M. C., & Carpenter, J. F. (1996). Infrared and circular dichroism spectroscopic characterization of structural differences between β-lactoglobulin A and B. *Biochemistry, 35*(5), 1450–1457. https://doi.org/10.1021/bi9518104.

Downham, A., & Collins, P. (2000). Colouring our foods in the last and next millennium. *International Journal of Food Science & Technology, 35*(1), 5–22. https://doi.org/10.1046/j.1365-2621.2000.00373.x.

Ebrahimi, S. E., Koocheki, A., Milani, E., & Mohebbi, M. (2016). Interactions between Lepidium perfoliatum seed gum – Grass pea (Lathyrus sativus) protein isolate in composite biodegradable film. *Food Hydrocolloids, 54*, 302–314. https://doi.org/10.1016/j.foodhyd.2015.10.020.

Ersus Bilek, S., Yılmaz, F. M., & Özkan, G. (2017). The effects of industrial production on black carrot concentrate quality and encapsulation of anthocyanins in whey protein hydrogels. *Food and Bioproducts Processing, 102*, 72–80. https://doi.org/10.1016/j.fbp.2016.12.001.

Fabek, H., Messerschmidt, S., Brulport, V., & Goff, H. D. (2014). The effect of invitro digestive processes on the viscosity of dietary fibres and their influence on glucose diffusion. *Food Hydrocolloids, 35*, 718–726. https://doi.org/10.1016/j.foodhyd.2013.08.007.

Fathi, M., Donsi, F., & McClements, D. J. (2018). Protein-based delivery systems for the nanoencapsulation of food ingredients. *Comprehensive Reviews in Food Science and Food Safety, 17*(4), 920–936. https://doi.org/10.1111/1541-4337.12360.

Fattahi, A., Petrini, P., Munarin, F., Shokoohinia, Y., Golozar, M. A., Varshosaz, J., ... Tanzi, M. C. (2013). Polysaccharides derived from tragacanth as biocompatible polymers and Gels. *Journal of Applied Polymer Science, 129*(4), 2092–2102. https://doi.org/10.1002/app.38931.

Ferreira, D. S., Faria, A. F., Grosso, C. R. F., & Mercadante, A. Z. (2009). Encapsulation of blackberry anthocyanins by thermal gelation of curdlan. *Journal of the Brazilian Chemical Society, 20*(10), 1908–1915.

García-Ochoa, F., Santos, V. E., Casas, J. A., & Gómez, E. (2000). Xanthan gum: Production, recovery, and properties. *Biotechnology Advances, 18*(7), 549–579. https://doi.org/10.1016/S0734-9750(00)00050-1.

Graf, B. A., Milbury, P. E., & Blumberg, J. B. (2005). Mini-review flavonols, flavones, flavanones, and human health: Epidemiological evidence. *Journal of Medicinal Food, 8*(3), 281–290.

Grunin, L., Oztop, M. H., Guner, S., & Baltaci, S. F. (2019). Exploring the crystallinity of

different powder sugars through solid echo and magic sandwich echo sequences. *Magnetic Resonance in Chemistry,* 0–1. https://doi.org/10.1002/mrc.4866.
Gunasekaran, S., Ko, S., & Xiao, L. (2007). Use of whey proteins for encapsulation and controlled delivery applications. *Journal of Food Engineering, 83*(1), 31–40. https://doi.org/10.1016/j.jfoodeng.2006.11.001.
Harnkarnsujarit, N., & Charoenrein, S. (2011). Effect of water activity on sugar crystallization and β-carotene stability of freeze-dried mango powder. *Journal of Food Engineering, 105*(4), 592–598. https://doi.org/10.1016/j.jfoodeng.2011.03.026.
Havea, P., Singh, H., & Creamer, L. K. (2001). A-lactalbumin and bovine serum albumin in a whey protein concentrate environment. *Journal of Dairy Research, 68*, 483–497.
Hoffman, M. A. M., & Van Mil, P. J. J. M. (1999). Heat-induced aggregation of β-lactoglobulin as a function of pH. *Journal of Agricultural and Food Chemistry, 47*(5), 1898–1905. https://doi.org/10.1021/jf980886e.
Hoffmann, M. A. M., & Van Mil, P. J. J. M. (1997). Heat-induced aggregation of β-lactoglobulin: Role of the free thiol group and disulfide bonds. *Journal of Agricultural and Food Chemistry, 45*(8), 2942–2948. https://doi.org/10.1021/jf960789q.
Jones, O. G., & McClements, D. J. (2010). Biopolymer nanoparticles from heat-treated electrostatic protein-polysaccharide complexes: Factors affecting particle characteristics. *Journal of Food Science, 75*(2), https://doi.org/10.1111/j.1750-3841.2009.01512.x.
Ju, Z. Y., & Kilara, A. (1998). Effects of preheating on properties of aggregates and of cold-set gels of whey protein isolate. *Journal of Agricultural and Food Chemistry, 46*(9), 3604–3608. https://doi.org/10.1021/jf980392h.
Kamiloglu, S., Pasli, A. A., Ozcelik, B., Van Camp, J., & Capanoglu, E. (2015). Influence of different processing and storage conditions on in vitro bioaccessibility of polyphenols in black carrot jams and marmalades. *Food Chemistry, 186*, 74–82. https://doi.org/10.1016/j.foodchem.2014.12.046.
Kammerer, D., Carle, R., & Schieber, A. (2004). Quantification of anthocyanins in black carrot extracts (Daucus carota ssp. sativus var. atrorubens Alef.) and evaluation of their color properties. *European Food Research and Technology, 219*(5), 479–486. https://doi.org/10.1007/s00217-004-0976-4.
Kirca, A., Ozkan, M., & Cemeroglu, B. (2006). Food chemistry stability of black carrot anthocyanins in various fruit juices and nectars. *Food Chemistry, 97*, 598–605. https://doi.org/10.1016/j.foodchem.2005.05.036.
Kitabatake, N., & Kinekawa, Y. I. (1998). Digestibility of bovine milk whey protein and β-lactoglobulin in vitro and in vivo. *Journal of Agricultural and Food Chemistry, 46*(12), 4917–4923. https://doi.org/10.1021/jf9710903.
Kodati, V. R., & Lafleur, M. (1993). Comparison between orientational and conformational orders in fluid lipid bilayers. *Biophysical Journal, 64*(1), 163–170. https://doi.org/10.1016/S0006-3495(93)81351-1.
Kurt, A. (2018). Physicochemical, rheological and structural characteristics of alcohol precipitated fraction of gum tragacanth. *Food and Health, 4*(3), 183–193. https://doi.org/10.3153/fh18019.
Lal, N., Dubey, J., Gaur, P., Verma, N., & Verma, A. (2017). Chitosan based in situ forming polyelectrolyte complexes: A potential sustained drug delivery polymeric carrier for high dose drugs. *Materials Science and Engineering C, 79*(May), 491–498. https://doi.org/10.1016/j.msec.2017.05.051.
Lefèvre, T., & Subirade, M. (1999). Structural and interaction properties of β-lactoglobulin as studied by FTIR spectroscopy. *International Journal of Food Science & Technology, 34*(5–6), 419–428. https://doi.org/10.1046/j.1365-2621.1999.00311.x.
Lowry, O. H., Rosebrough, N. J., Farr, A. L., & Randall, R. J. (1951). The folin by oliver. *The Journal of Biological Chemistry, 275*, 265–275. Retrieved from http://linkinghub.elsevier.com/retrieve/pii/S0003269784711122.
Manetti, C., Casciani, L., & Pescosolido, N. (2004). LF-NMR water self-diffusion and relaxation time measurements of hydrogel contact lenses interacting with artificial tears. *Journal of Biomaterials Science Polymer Edition, 15*(3), 331–342. https://doi.org/10.1163/156856204322977210.
Maus, A., Hertlein, C., & Saalwächter, K. (2006). A robust proton NMR method to investigate hard/soft ratios, crystallinity, and component mobility in polymers. *Macromolecular Chemistry and Physics, 207*(13), 1150–1158. https://doi.org/10.1002/macp.200600169.
McClements, D. J., & Gumus, C. E. (2016). Natural emulsifiers-Biosurfactants, phospholipids, biopolymers and colloidal particles: Molecular and physicochemical basis of functional performance. *Advances in Colloid and Interface Science, 234*, 3–26. https://doi.org/10.1016/j.cis.2016.03.002.
McDougall, G. J., Dobson, P., Smith, P., Blake, A., & Stewart, D. (2005). Assessing potential bioavailability of raspberry anthocyanins using an in vitro digestion system. *Journal of Agricultural and Food Chemistry, 53*(15), 5896–5904. https://doi.org/10.1021/jf050131p.
Metzger, B. T., & Barnes, D. M. (2009). Polyacetylene diversity and bioactivity in orange market and locally grown colored carrots (Daucus carota L). *Journal of Agricultural and Food Chemistry, 57*(23), 11134–11139. https://doi.org/10.1021/jf9025663.
Mikac, U., Sepe, A., Kristl, J., & Baumgartner, S. (2010). A new approach combining different MRI methods to provide detailed view on swelling dynamics of xanthan tablets influencing drug release at different pH and ionic strength. *Journal of Controlled Release, 145*(3), 247–256. https://doi.org/10.1016/j.jconrel.2010.04.018.
Mohnen, D. (2008). Pectin structure and biosynthesis. *Current Opinion in Plant Biology, 11*(3), 266–277. https://doi.org/10.1016/j.pbi.2008.03.006.
Mostafavi, F. S., Kadkhodaee, R., Emadzadeh, B., & Koocheki, A. (2016). Preparation and characterization of tragacanth – Locust bean gum edible blend films. *Carbohydrate Polymers, 139*, 20–27. https://doi.org/10.1016/j.carbpol.2015.11.069.
Munialo, D. C., Linden, E., Van Der Ako, K., Nieuwland, M., Van As, H., & De Jongh, H. H. J. (2016). The effect of polysaccharides on the ability of whey protein gels to either store or dissipate energy upon mechanical deformation. *Food Hydrocolloids, 52*, 707–720. https://doi.org/10.1016/j.foodhyd.2015.08.013.
Naczk, M., Grant, S., Zadernowski, R., & Barre, E. (2006). Protein precipitating capacity of phenolics of wild blueberry leaves and fruits. *Food Chemistry, 96*(4), 640–647. https://doi.org/10.1016/j.foodchem.2005.03.017.
Nur, M., Ramchandran, L., & Vasiljevic, T. (2016). Tragacanth as an oral peptide and protein delivery carrier: Characterization and mucoadhesion. *Carbohydrate Polymers, 143*, 223–230. https://doi.org/10.1016/j.carbpol.2016.01.074.
Ozel, B., Aydin, O., Grunin, L., & Oztop, M. H. (2018). Physico-chemical changes of composite whey protein hydrogels in simulated gastric fluid conditions. *Journal of Agricultural and Food Chemistry, 66*(36), 9542–9555. https://doi.org/10.1021/acs.jafc.8b02829 research-article.
Ozel, B., Cikrikci, S., Aydin, O., & Oztop, M. H. (2017). Polysaccharide blended whey protein isolate-(WPI) hydrogels: A physicochemical and controlled release study. *Food Hydrocolloids, 71*, 35–46. https://doi.org/10.1016/j.foodhyd.2017.04.031.
Oztop, M. H., McCarthy, K. L., McCarthy, M. J., & Rosenberg, M. (2014). Monitoring the effects of divalent ions (Mn + 2 and Ca + 2) in heat-set whey protein gels. *LWT - Food Science and Technology, 56*(1), 93–100. https://doi.org/10.1016/j.lwt.2013.10.043.
Oztop, M. H., Rosenberg, M., Rosenberg, Y., McCarthy, K. L., & McCarthy, M. J. (2010). Magnetic resonance imaging (MRI) and relaxation spectrum analysis as methods to investigate swelling in whey protein gels. *Journal of Food Science, 75*(8), 508–515. https://doi.org/10.1111/j.1750-3841.2010.01788.x.
Pakzad, H., Alemzadeh, I., & Kazemi, A. (2013). Encapsulation of peppermint oil with arabic gum-gelatin by complex coacervation method. *International Journal of Engineering, Transactions B: Applications, 26*(8), 807–814. https://doi.org/10.5829/idosi.ije.2013.26.08b.01.
Pérez, L. M., Piccirilli, G. N., Delorenzi, N. J., & Verdini, R. A. (2016). Effect of different combinations of glycerol and/or trehalose on physical and structural properties of whey protein concentrate-based edible films. *Food Hydrocolloids, 56*, 352–359. https://doi.org/10.1016/j.foodhyd.2015.12.037.
Pocan, P., Ilhan, E., & Oztop, M. H. (2019). Characterization of emulsion stabilization properties of gum tragacanth, xanthan gum and sucrose monopalmitate: A comparative study. *Journal of Food Science, 84*(5), 1087–1093. https://doi.org/10.1111/1750-3841.14602.
Prabakaran, S., & Damodaran, S. (1997). Thermal unfolding of β-lactoglobulin: Characterization of initial unfolding events responsible for heat-induced aggregation. *Journal of Agricultural and Food Chemistry, 45*(11), 4303–4308. https://doi.org/10.1021/jf970269a.
Ralet, M.-C., Dronnet, V., Buchholt, H. C., & Thibault, J.-F. (2011). Enzymatcally and chemically de-esterified lime pectins: Physico-chemical characterisation, polyelectrolyte behaviour and calcium binding properties. *Carbohydrate Research, 336*, 117–125. https://doi.org/10.1039/9781847551672-00055.
Rhim, W. K., Pines, A., & Waugh, J. S. (1971). Time-reversal experiments in dipolar-coupled spin systems. *Physical Review B, 3*, 684–696.
Saldamli, I. (1998). In I. Saldamli (Ed.). *Gida kimyasi.* Ankara: Hacettepe University Press.
Sánchez-García, Y. I., Gutiérrez-Méndez, N., Orozco-Mena, R. E., Ramos-Sánchez, V. H., & Leal-Ramos, M. Y. (2019). Individual and combined effect of pH and whey proteins on lactose crystallization. *Food Research International, 116*(January 2018), 455–461. https://doi.org/10.1016/j.foodres.2018.08.061.
Santipanichwong, R., Suphantharika, M., Weiss, J., & McClements, D. J. (2008). Core-shell biopolymer nanoparticles produced by electrostatic deposition of beet pectin onto heat-denatured β-lactoglobulin aggregates. *Journal of Food Science, 73*(6), https://doi.org/10.1111/j.1750-3841.2008.00804.x.
Sarkar, A., Goh, K. K. T., Singh, R. P., & Singh, H. (2009). Behaviour of an oil-in-water emulsion stabilized by β-lactoglobulin in an in vitro gastric model. *Food Hydrocolloids, 23*(6), 1563–1569. https://doi.org/10.1016/j.foodhyd.2008.10.014.
Souza, F. N., Gebara, C., Ribeiro, M. C. E., Chaves, K. S., Gigante, M. L., & Grosso, C. R. F. (2012). Production and characterization of microparticles containing pectin and whey proteins. *Food Research International, 49*(1), 560–566. https://doi.org/10.1016/j.foodres.2012.07.041.
Stein, W. H., & Moore, S. (1949). Amino acid composition of beta lactoglobulin and bovine serum albumin. *The Journal of Biological Chemistry, 178*, 79–91.
Stintzing, F. C., Stintzing, A. S., Carle, R., Frei, B., & Wrolstad, R. E. (2002). Color and antioxidant properties of cyanidin-based anthocyanin pigments. *Journal of Agricultural and Food Chemistry, 50*(21), 6172–6181. https://doi.org/10.1021/jf0204811.
Su, J. F., Huang, Z., Yuan, X. Y., Wang, X. Y., & Li, M. (2010). Structure and properties of carboxymethyl cellulose/soy protein isolate blend edible films crosslinked by Maillard reactions. *Carbohydrate Polymers, 79*(1), 145–153. https://doi.org/10.1016/j.carbpol.2009.07.035.
Tagliazucchi, D., Verzelloni, E., Bertolini, D., & Conte, A. (2010). In vitro bio-accessibility and antioxidant activity of grape polyphenols. *Food Chemistry, 120*(2), 599–606. https://doi.org/10.1016/j.foodchem.2009.10.030.
Takagi, K., Teshima, R., Okunuki, H., & Sawada, J. (2003). Comparative study of in vitro digestibility of food proteins and effect of preheating on the digestion. *Biological & Pharmaceutical Bulletin, 26*(7), 969–973. https://doi.org/10.1248/bpb.26.969.
Tanford, C., Bunville, L. G., & Nozaki, Y. (1959). The reversible transformation of β-lactoglobulin at pH 7.5. *Journal of the American Chemical Society, 81*(15), 4032–4036. https://doi.org/10.1021/ja01524a054.
Turgeon, S. L., & Beaulieu, M. (2001). Improvement and modification of whey protein gel texture using polysaccharides. *Food Hydrocolloids, 15*(4–6), 583–591. https://doi.org/10.1016/S0268-005X(01)00064-9.
Urias-Orona, V., Rascón-Chu, A., Lizardi-Mendoza, J., Carvajal-Millán, E., Gardea, A. A., & Ramírez-Wong, B. (2010). A novel pectin material: Extraction, characterization and gelling properties. *International Journal of Molecular Sciences, 11*(10), 3686–3695. https://doi.org/10.3390/ijms11103686.
Ventura, I., & Bianco-Peled, H. (2015). Small-angle X-ray scattering study on pectin-chitosan mixed solutions and thermoreversible gels. *Carbohydrate Polymers, 123*, 122–129. https://doi.org/10.1016/j.carbpol.2015.01.025.

Vittadini, E., Dickinson, L. C., & Chinachoti, P. (2002). NMR water mobility in xanthan and locust bean gum mixtures: Possible explanation of microbial response. *Carbohydrate Polymers, 49*(3), 261–269. https://doi.org/10.1016/S0144-8617(01)00330-7.

Wang, H., Gao, X. D., Zhou, G. C., Cai, L., & Yao, W. B. (2008). In vitro and in vivo antioxidant activity of aqueous extract from Choerospondias axillaris fruit. *Food Chemistry, 106*(3), 888–895. https://doi.org/10.1016/j.foodchem.2007.05.068.

Wang, Y. W., Chen, L. Y., An, F. P., Chang, M. Q., & Song, H. B. (2018). A novel polysaccharide gel bead enabled oral enzyme delivery with sustained release in small intestine. *Food Hydrocolloids, 84*(May), 68–74. https://doi.org/10.1016/j.foodhyd.2018.05.039.

Xu, M., & Dumont, M. J. (2015). Evaluation of the stability of pea and canola protein-based hydrogels in simulated gastrointestinal fluids. *Journal of Food Engineering, 165*, 52–59. https://doi.org/10.1016/j.jfoodeng.2015.04.033.

Yang, H., Li, J. G., Wu, N. F., Fan, M. M., Shen, X. L., Chen, M. T., ... Lai, L. S. (2015). Effect of hsian-tsao gum (HG) content upon rheological properties offilm-forming solutions (FFS) and physical properties of soy protein/hsian-tsao gum films. *Food Hydrocolloids, 50*, 211–218. https://doi.org/10.1016/j.foodhyd.2015.03.028.

Yildiz, F. (2010). In F. Yildiz (Ed.). *Advances in food biochemistry*(1st ed.). New York: CRC Press.

Yokoyama, A., Srinivasan, K. R., & Fogler, H. S. (1988). Stabilization mechanism of colloidal suspensions by Gum Tragacanth.pdf. *Journal of Colloid and Interface Science, 126*(1), 141–149.

Zand-Rajabi, H., & Madadlou, A. (2016). Caffeine-loaded whey protein hydrogels reinforced with gellan and enriched with calcium chloride. *International Dairy Journal, 56*, 38–44. https://doi.org/10.1016/j.idairyj.2015.12.011.

Zhang, M. P., Yang, Z. C., Chow, L. L., & Wang, C. H. (2003). Simulation of drug release from biodegradable polymeric microspheres with bulk and surface erosions. *Journal of Pharmaceutical Sciences, 92*(10), 2040–2056. https://doi.org/10.1002/jps.10463.

Zhang, S., Zhang, Z., & Vardhanabhuti, B. (2014). Effect of charge density of polysaccharides on self-assembled intragastric gelation of whey protein/polysaccharide under simulated gastric conditions. *Food & Function, 5*(8), 1829–1838. https://doi.org/10.1039/C4FO00019F.